GAMESMITH: SCALING ZERO-SUM SELF-PLAY WITH SYNTHESISED GAMES

Anonymous authors
Paper under double-blind review

ABSTRACT

Post-training large language models (LLMs) on two-player zero-sum games provides a verifiable reward, and the gains have been shown to transfer to general reasoning. Existing pipelines, however, rely on a handful of hand-written games and on advantage estimators tied to them, so both the supply of games and the advantage estimate on a large corpus limit scaling. We present GAMESMITH, which scales both. An LLM synthesises games inside templates whose reward, observation, and hidden-information code is fixed. Each game is verified by seed-paired replay and by an independent re-implementation of its specification, then expanded into encoding, rule, and size variants, giving 26 new games in 29 families and 336 verified variants from the three SPIRAL templates. The model is distilled from the self-play of a larger teacher (Qwen3-32B) on these games and then trained by self-play reinforcement learning with CRAB, an advantage estimator that credits each decision against a shrinkage estimate of the expected return of its position and is defined on every variant. On Qwen3-4B-Base, distillation raises the 13-benchmark mean pass@1 from 45.5 to 62.5, above the three SPIRAL games at the same budget, and self-play with CRAB reaches 64.9. The ordering holds across models, and transfer grows with the number of game families.

1 INTRODUCTION

Two-player zero-sum games are an attractive source of post-training data for large language models (LLMs), for three reasons: (1) the outcome of every game (win, loss, or draw), is computed by the game engine and serves as the reward, so the reward is verifiable; (2) trajectories are generated by game play, so their supply is unbounded; and (3) because the same model plays both sides, the opponent improves together with it, which naturally leads to a curriculum process (Silver et al., 2018; Baker et al., 2020). Post-training on games has been shown to transfer to mathematical and general reasoning (Cheng et al., 2024; Liu et al., 2026; Yuan et al., 2026). SPIRAL (Liu et al., 2026) and MARSHAL (Yuan et al., 2026) demonstrate this with multi-turn self-play on three hand-written text games, and both identify the supply of new games as their limiting factor. More broadly, across reinforcement learning (RL) on verifiable tasks, adding environments improves generalisation more reliably than adding compute on a fixed set (Stojanovski et al., 2026; Zeng et al., 2026).

Scaling game-based post-training, therefore, has two-fold requirements: (1) supply of games without relying on human labour. Although LLMs are able to write game code (Verma et al., 2025; Faldor et al., 2025; Song et al., 2026), existing pipelines check only that the generated code executes, not that it implements the intended game. Executability alone guarantees neither a correct implementation nor a trustworthy reward; and (2) post-training that scales as the number of games grows, since under fixed budgets, the visits to a single game become sparse. Existing self-play methods estimate the advantage baseline separately for each game from its past returns (Liu et al., 2026), which rely on repeated playing on individual games.

In this paper, we present GAMESMITH, a framework that retains the setting of SPIRAL, namely multi-turn self-play on two-player zero-sum text games, and scales it on both fronts. To the best of our knowledge, GAMESMITH is the first method in the literature that scales LLM post-training by self-play on synthesised two-player zero-sum games.

To scale the supply of games (Figure 1), an LLM synthesises games inside *templates*: the generated code fills in game-specific functions, while the code that assigns the reward, builds observations, and

Reviewers: please read the Reviewer Guidelines (iclr.cc/Conferences/2027/ReviewerGuidelines) and the AI Policy for Reviewers (iclr.cc/Conferences/2027/AIPolicyForReviewers). If you used AI to expand, edit, or polish your review, please provide the input text to the LLM. Better still, consider skipping the LLM and submitting your original text: we, and the authors, are much more interested in your unedited thoughts than in what an LLM has to say. AI-assisted or not, you are putting your name and reputation behind your review: LLM-generated falsehoods, hallucinations or misrepresentations are subject to disciplinary action, which may include desk-rejecting all papers you have authored.

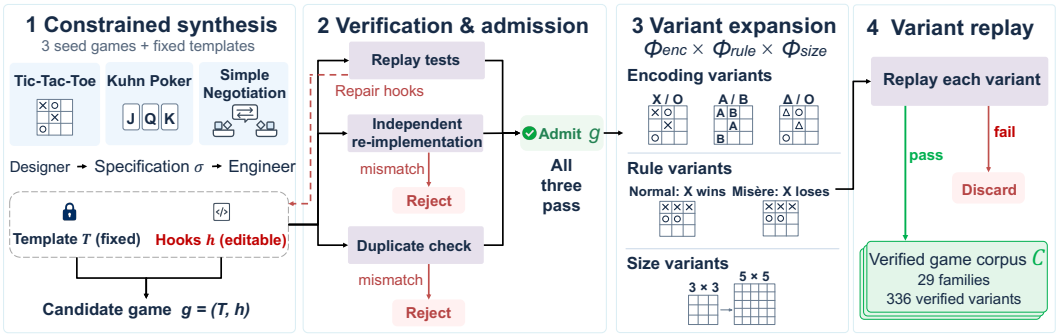

Figure 1: The GAMESMITH game supply: an LLM fills the hooks of a fixed template, the game is admitted after replay tests, an independent re-implementation, and a duplicate check, and its encoding, rule, and size variants are replayed before entering the corpus.

routes hidden information is fixed, so that these properties cannot be corrupted. The generated game logic is verified before use and then expanded into variants of its encoding, rules, and size. Building on the three templates derived from the SPIRAL games, this procedure creates 26 new games in 29 families, with 163 rule and size variants (86 and 77) and 173 encoding variants.

To scale post-training (Figure 2), GAMESMITH trains its model in two stages, both using self-play trajectories from the synthesised games: (1) supervised fine-tuning on the self-play of a larger teacher model, Qwen3-32B, which plays the synthesised games against itself, followed by (2) reinforcement learning on the model's own self-play. For the second stage, we introduce CRAB, a baseline for the policy-gradient estimate, i.e., the quantity subtracted from each return to reduce variance, that is defined on every corpus variant. CRAB combines two estimates of the expected return of a game: the returns of the same game in the current batch, and a prior fitted across the corpus. The two are weighted as a Bayes estimator, and a state value computed by the template is then added for each position. Since it does not depend on the taken action, the policy-gradient estimate remains unbiased for the self-play objective. Further, under a standard uncorrelatedness assumption, its per-episode variance is lower than with either source alone.

We evaluate GAMESMITH on 13 reasoning benchmarks in mathematics, knowledge, logical reasoning, and spatial and state tracking. Distillation from the synthesised games raises Qwen3-4B-Base from 45.5 to 62.5 (mean pass@1 over four samples per question), outperforming both the same token budget of the three SPIRAL games (60.6) and the same teacher on budget-matched non-game reasoning data (60.8). Self-play RL with CRAB then further improves the average to 64.9, outperforming the RAE algorithm proposed in SPIRAL.

2 RELATED WORK

Post-training on games. Self-play on games is the classic route to strong play (Silver et al., 2016; 2018), and games have also been used to measure the strategic reasoning of LLMs (Duan et al., 2024; Costarelli et al., 2024; Bianchi et al., 2024). As a source of post-training data, SPAG trains a policy through adversarial word games (Cheng et al., 2024), SPIRAL runs multi-turn zero-sum self-play on hand-written text games (Liu et al., 2026), and MARSHAL extends this setting to several games (Yuan et al., 2026). All of these train on between one and six authored games and identify the supply of games as the bottleneck. A parallel line of work has the model write its own training problems and rewards it through code execution or agreement among its samples (Zhao et al., 2025; Huang et al., 2026; Liu et al., 2025a; Zhou et al., 2025; Chen et al., 2025b), with self-play versions that pit a proposer against a solver or a critic (Kuba et al., 2025; Chen et al., 2025a), and self-training retains the model's own samples that pass a verifier or a consistency check (Zelikman et al., 2022; Singh et al., 2024; Yuan et al., 2024; Shafayat et al., 2025; Li et al., 2023). In game post-training, the reward is the outcome of the game, which the proposer cannot manipulate.

Environment generation and variation. LLMs have been used to generate games and tasks as benchmarks (Verma et al., 2025), as open-ended task pools (Faldor et al., 2025), and as procedurally defined RL environments (Matthews et al., 2025; Stojanovski et al., 2026). Recent work further

reports that the number of verifiable environments, rather than compute on a fixed set, is what drives generalisation (Zeng et al., 2026; Song et al., 2026; Wang et al., 2026; Dong et al., 2026; Li et al., 2026b). The closest to our setting is GG-Bench (Verma et al., 2025), where an LLM writes two-player games and 126 of 1,000 survive filters for execution, run time, and beatability by a trained agent, while the agreement between an implementation and its description is inspected by hand on ten of them. Generated environments have also been used for training: Zhou et al. (2026) post-train a code generator by self-distillation on projects that pass an execution gate, Shi et al. (2026) train a single policy by reinforcement learning on reasoning environments that it synthesises itself, admitted by execution, difficulty, and novelty checks, and Jia et al. (2026) verify generated games by reaching keypoints of the state from injected states. None of these involves two-player zero-sum games or self-play, and none checks an implementation against a second, independent reading of its specification. Unsupervised environment design and domain randomisation vary a single level space to improve robustness (Dennis et al., 2020; Wang et al., 2019; Tobin et al., 2017), and procedural benchmarks measure generalisation across levels (Cobbe et al., 2019).

Advantage baselines. Policy-gradient post-training of LLMs (Schulman et al., 2017; Ouyang et al., 2022; DeepSeek-AI, 2025; Li et al., 2026a) typically uses group or leave-one-out baselines over samples of the same prompt (Shao et al., 2024; Ahmadian et al., 2024; Liu et al., 2025b; Yu et al., 2025) or learned value estimates (Kazemnejad et al., 2025). In game self-play, the analogue of a prompt is a pair of a variant and a seat, and SPIRAL maintains one running mean per such pair (Liu et al., 2026).

3 PRELIMINARIES

Games. This paper studies two-player, turn-based, finite-horizon games with a zero-sum outcome: either one player wins and the other loses, or the game is drawn. The two positions a player can take are the *seats* $o \in \{0, 1\}$, where seat 0 moves first. The *trajectory* τ of a seat in an *episode*, a single play of a game from start to end, is the sequence of observations and actions that the seat received and took, and its *return* $R(\tau) \in \{+1, 0, -1\}$ is the outcome from that seat's point of view, as computed by the game engine. A *policy* maps an observation to a distribution over actions. We denote by π_θ the model being trained and by π_{T} the teacher from whose self-play it is distilled.

Variants. A *descriptor* $\phi = (\phi^{\mathrm{enc}}, \phi^{\mathrm{rule}}, \phi^{\mathrm{size}})$ specifies three components. The *encoding* ϕ^{enc} determines how a state is written (e.g., the marks, coordinate scheme, and orientation of a Tic-Tac-Toe board), and it changes the text but not the game. The *rules* ϕ^{rule} consist of a legality, transition, or outcome clause, such as forbidding the centre on the first move, and they change the game. The *size* ϕ^{size} specifies the size of the state and action spaces, such as a 5×5 board, and it changes the game while keeping its rules. A *variant* E_ϕ is the game fixed to a descriptor, the *family* of a game is the set of its admitted variants, and the *corpus* is the union of all families. We write $\psi(\phi) = (\phi^{\mathrm{rule}}, \phi^{\mathrm{size}})$ for the part of a descriptor that changes the game. Encodings leave the game unchanged, but the model reads text and must learn this invariance from the renderings it observes, which is why they form a separate axis (Appendix B.3 and B.4).

Policy gradient with a baseline. In self-play the same policy occupies both seats, and the update treats each seat in turn as the learner, with the opponent's actions held fixed as part of the environment. The objective of the learning seat is its expected return $J(\theta) = \mathbb{E}[R(\tau)]$ over variants and over trajectories τ of that seat, drawn from π_θ against a copy of the current policy through which no gradient is taken, and the update sums the gradients of the two seats. The objective is defined per seat because the return averaged over both seats of a zero-sum game is identically zero. Given a batch of N seat trajectories τ_i, the gradient is estimated by

$$\hat{g} \;=\; \frac{1}{N} \sum_{i=1}^{N} \big(R(\tau_i) - b_i\big)\, \nabla_\theta \log \pi_\theta(\tau_i), \tag{1}$$

where the *baseline* b_i is any quantity that does not depend on the actions in τ_i. Such a baseline leaves the estimate unbiased and affects only its variance (Ahmadian et al., 2024; Liu et al., 2025b), and the variance is minimised when b_i is closest in mean squared error to the expected return of the game and seat of episode i (Appendix B.1). In game self-play, b_i must depend on the seat, since

most games favour the first mover, and it must also be defined for every variant of a large corpus, most of which a run visits only a few times. RAE, the estimator of Liu et al. (2026), maintains a running mean return per variant and seat and uses the corresponding cell as b_i.

4 METHOD

GAMESMITH scales game-based post-training on two fronts (Figures 1 and 2). On the data side, a synthesis pipeline lets an LLM write new zero-sum games and admits only those that pass verification (§4.1). On the post-training side, the resulting corpus has hundreds of variants that a run visits only a few times, which breaks the per-game advantage baselines of existing self-play methods, so we propose CRAB, a baseline that is defined on every variant of the corpus (§4.2).

4.1 SCALING THE SUPPLY OF GAMES: SYNTHESIS WITH VERIFICATION

Templates. A *template* $T = (K, H)$ consists of a *kernel* K, which is code that is fixed for every game built on the template, and a *hook set* $H = \{h_1, \ldots, h_m\}$, which is the set of named functions that a game must supply. The kernel encodes observations, assigns rewards, and builds each seat's observation from the state, whereas the hooks return only game-specific verdicts: whether an action is legal, the next state, and who has won. A game is thus a template together with an implementation of its hooks, $g = (T, h)$. We use 3 templates, one per genre, each seeded by one of the three SPIRAL games (Liu et al., 2026): grid placement with perfect information, betting with a showdown under imperfect information, and resource negotiation under private valuations. Each template has between one and four hooks (Appendix A.1) and settles every game as zero-sum.

Because the kernel is fixed, every game on a template has a zero-sum reward structure consistent with the hooks' verdicts. Hidden state reaches each seat only through the channels declared by the kernel Encoding variants differ only in their text, since the kernel itself applies the bijection e (§3).

Generation. Games are written by two LLM roles. A *designer* writes a specification consisting of the rules in natural language, the semantic parameters (e.g., board size, deck, code length), and the deductive skill that the game should exercise. An *engineer* then implements the specification by filling in the hooks of the corresponding template, and it cannot modify the kernel. When a test fails, its output is returned to the engineer for revision, and a game that exhausts its bounded number of repair attempts is discarded (Appendix E gives the models, decoding, and prompts).

Verification. Every test is built on a single primitive, *seed-paired replay*: two environments are run from the same random seed under the same driver, i.e., a policy that supplies actions to both, and a relation between the two trajectories is checked on every seed of a fixed set (Appendix A.2 states each test formally as a predicate, and Appendix A.3 reports which injected defects each test catches). Two tests have a known answer because of the kernel: an encoding variant must have identical outcomes once actions are mapped through e, and a rule variant must change the outcome on at least one seed. Three further tests check termination and zero-sum rewards, information hiding under perturbation of the hidden state, and playability under a reference bot (Table 4).

Replay tests have not yet checked that the implementation is the game that the designer described, so a second model from a different model family implements the same specification without access to the first implementation, and the two implementations are replayed from shared seeds under the same driver. Any disagreement on an outcome leads to rejection of the game (Appendix A.3 also compares ten admitted games with their specifications by hand). Finally, a game whose play statistics under the random driver are close to those of an already admitted game is replayed against it from shared seeds, and it is rejected as a duplicate if the outcomes match on every seed. A game is admitted when it passes every replay test, agrees with its re-implementation, and is not a duplicate. An LLM playtest then scores each admitted game on playability from the rules text alone, as a diagnostic that plays no role in admission.

Variant expansion. Each admitted game is expanded into its family. The descriptor set is the product of three per-component sets,

$$\Phi(g) = \Phi_{\mathrm{enc}}(g) \times \Phi_{\mathrm{rule}}(g) \times \Phi_{\mathrm{size}}(g), \tag{2}$$

where encodings are enumerated from the template's pools, rule variants are typed perturbations of the semantic parameters, and size variants change the state and action spaces. Every variant must itself pass the replay tests. Moreover, every rule and size variant is annotated with an *effect size*, defined as the fraction of seed-paired episodes whose outcome differs between the variant and its parent. The variants used at each training stage are listed in Appendix A.4.2.

4.2 Scaling post-training: distillation and self-play with CRAB

The model is distilled from a teacher's self-play on the corpus and then trained by self-play RL, whose advantage baseline must be defined on every variant of a corpus that a run visits only a few times. We describe the distillation stage, then this baseline, and then the self-play stage.

Distillation. The teacher π_{T} plays variants of every family against itself. Each decision is recorded as a prompt (rules text, current observation, and action format) and a response (a reasoning block followed by the chosen action). The student π_θ is then fine-tuned on these records.

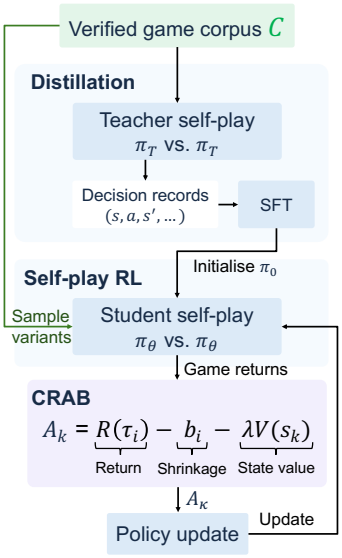

Figure 2: Post-training on the verified corpus with CRAB.

Shrinkage baseline. CRAB, a corpus-regularised advantage baseline, serves as the b_i in equation 1: it estimates the expected return of the game and seat of episode i as a Bayes estimator that combines the information in the current batch with that of the rest of the corpus.

This quantity is keyed on what a variant is rather than on its identity. The *group* of an episode is $g = (\psi(\phi), o)$, i.e., the components of the descriptor that change the game, together with the seat. The encoding is excluded because it is redrawn every episode and does not change the game (§3). Consequently, the returns of one group are the returns of one game from one seat, averaged over its encodings. Let μ_g denote the expected return of group g under the current policy. At each optimiser step, two sources of information about μ_g are available. The first is the batch itself. Because each sampled variant is played G times (§4.2), the batch contains $K_g \geq G$ episodes of group g, and the leave-one-out mean

$$\bar{y}_{g,-i} \;=\; \frac{1}{K_g - 1} \sum_{j \in g,\, j \neq i} R(\tau_j) \tag{3}$$

is an unbiased estimate of μ_g under the current policy, with variance $\sigma^2/(K_g - 1)$, where σ^2 is the variance of a single return. The second is a *prior* m_g, which is a linear model on the descriptor with one weight per value of each rule and size field, one weight per seat, and an intercept, fitted by online least squares on the returns of all earlier batches. The prior is defined for every descriptor in the corpus, including combinations of field values that no episode has visited, but it lags behind the policy and cannot express interactions between fields.

CRAB combines the two sources as

$$b_i \;=\; \frac{K'_g\, \bar{y}_{g,-i} \;+\; \kappa\, m_g}{K'_g + \kappa}, \qquad K'_g = K_g - 1, \tag{4}$$

where $\kappa > 0$ is a pseudo-count that controls the weight of the prior. If the group means are modelled as $\mu_g \sim \mathcal{N}(m_g, \tau^2)$ and the returns of a group are modelled as independent with variance σ^2 about μ_g, then equation 4 with $\kappa = \sigma^2/\tau^2$ is the posterior mean of μ_g given the other returns of the group. Without the normality assumption, it remains the linear estimator of μ_g with the smallest mean squared error given the same two moments. Intuitively, a group with many episodes in the batch ($K'_g \gg \kappa$) relies on its own mean, whereas a group with few episodes falls back on the prior. As $\kappa \to 0$, b_i reduces to the leave-one-out mean of RLOO (Ahmadian et al., 2024) restricted to episodes of the same game and seat. As $\kappa \to \infty$, b_i reduces to the prior alone. RAE corresponds to neither: its table has one cell per variant and seat, so it pools no information across variants.

The main runs fix $\kappa = 4$, so that with $G = 5$ the batch mean and the prior receive equal weight. The model also prescribes κ: σ^2 and $\tau^2 = \mathbb{E}[(\mu_g - m_g)^2]$ are estimated from the returns of each batch, and $\hat{\kappa} = \hat{\sigma}^2/\hat{\tau}^2$ is recorded for every run, together with $\hat{\tau}^2_{\text{enc}}$, the same variance across encodings within a group, which is zero for an equivariant policy (Appendix B.2 gives the estimators, a variant of CRAB that uses $\hat{\kappa}$, and the error analysis).

The baseline b_i depends only on the other episodes of the batch and on a prior fitted before the batch, and not on the actions of τ_i. Therefore, equation 1 remains unbiased for any κ, whether fixed or estimated with lag. Its variance is governed by how well b_i estimates μ_g.

Lemma 1. *Let $\hat{g}_i = (R(\tau_i) - b_i)\nabla_\theta \log \pi_\theta(\tau_i)$ be the term of equation 1 contributed by episode i, and assume that the squared norm of the score $\nabla_\theta \log \pi_\theta(\tau_i)$ is uncorrelated with the squared return residual $(R(\tau_i)-b_i)^2$, which is the assumption under which the variance-minimising constant baseline is the expected return. Then $\mathrm{Var}[\hat{g}_i]$ is an increasing affine function of $\mathbb{E}[(b_i-\mu_g)^2]$. Under the model above, this error equals $\sigma^2/(K'_g + \kappa^\star)$ at $\kappa^\star = \sigma^2/\tau^2$, which is smaller than both the error σ^2/K'_g of the leave-one-out mean alone and the error τ^2 of the prior alone.*

The proof is given in Appendix B.1. Under the stated assumption, the estimator therefore reduces the variance of each gradient term relative to both of its limiting cases when κ is close to σ^2/τ^2, which is precisely the value that $\hat{\kappa}$ targets.

Self-play. In the second stage, the distilled model π_θ plays against a copy of itself. Each optimiser step samples variants and plays each one G times with fresh seeds. The encoding is drawn afresh for every episode and held fixed within the episode, so that a batch contains G episodes of every sampled game under different encodings. A drawn episode returns 0 to both seats and is treated as a sample of equation 1 like any other, and draws remain rare on the corpus (Appendix D.6). The policy is updated with equation 1, where the k-th decision of τ_i, taken in state s_k, receives the advantage

$$A_k \;=\; R(\tau_i) \;-\; b_i \;-\; \lambda\, V(s_k), \tag{5}$$

with b_i given by equation 4, $V(s_k) \in [-1, 1]$ a value of position s_k for the seat to move, which is a fixed function of the information visible to that seat that the template computes from its own hooks (Appendix A.1 defines it for each template), and $\lambda > 0$ a fixed weight. Both terms are absolute levels: b_i is the expected return of the game from this seat and $V(s_k)$ the value of the position under a fixed reference behaviour, which varies within the episode. Neither term depends on the action taken at decision k, so $b_i + \lambda V(s_k)$ is an action-independent baseline for that decision, and equation 5 keeps the gradient unbiased for any V.

5 EXPERIMENTS

We conducted extensive experiments addressing four research questions. **RQ1:** At a fixed teacher and token budget, does distillation from synthesised games transfer to general reasoning better than distillation from the three SPIRAL games, from non-game reasoning data, or from game data with the reasoning removed? **RQ2:** Does self-play on the synthesised corpus improve on the distilled model, does the full pipeline exceed the SPIRAL pipeline, and does CRAB improve on RAE? **RQ3:** How does transfer scale with the number of game families and with the number of trajectories? **RQ4:** Which properties of the corpus and which capabilities of the model account for the transfer?

5.1 IMPLEMENTATION DETAILS

Corpus. The corpus is seeded by the three games of SPIRAL (Liu et al., 2026), implemented on TextArena (Guertler et al., 2025), with one game per template: Tic-Tac-Toe, Kuhn Poker, and Simple Negotiation. The synthesiser admits 26 new games, resulting in 29 families with 163 rule and size variants that change the game (86 and 77) and 173 encoding variants that do not (Appendix A.4.1).

Models. Our main model is Qwen3-4B-Base (Yang et al., 2025), and the main comparisons are repeated on Qwen3-8B-Base and on two instruct models from other families, Mistral-Nemo-Instruct-2407 and GLM-4-9B-0414 (GLM, 2024). The teacher for every distillation setting is Qwen3-32B.

Pipeline. Distillation data are built as in §4.2, with the action in `\boxed`, and self-play with CRAB then starts from the distilled checkpoint. The hyperparameters, hardware, software, and compute are described in Appendices C.2 and C.3.

Implementations. All distillation settings share the same teacher, decoding configuration, output format, and token budget, and differ only in the environments that the teacher plays. SPIRAL distills from the three SPIRAL games only and serves as the main baseline. For GAMESMITH, we subsample our corpus to the same token budget as the baselines (8,208 trajectories). Non-game uses the same teacher on non-game reasoning problems (deductive logic, spatial and state tracking, and competition mathematics) at the same budget, decontaminated against every evaluation set (Appendix C.1). Format keeps the GAMESMITH prompts and the boxed action but removes the reasoning. For self-play RL, the SPIRAL pipeline runs the same two stages on the three SPIRAL games with RAE, the estimator of Liu et al. (2026), which amounts to SPIRAL with a distillation stage in front. The estimator control keeps the GAMESMITH corpus and checkpoint, the group size $G = 5$, and the token budget, and replaces CRAB with RAE.

Evaluation. We report pass@1 over 4 samples per question with an 8,192-token generation budget (Appendix C.4) on 13 benchmarks in four groups: mathematics (MATH-500 (Hendrycks et al., 2021; Lightman et al., 2024), AIME (Sun et al., 2026), AMC[1], Minerva Math (Lewkowycz et al., 2022), and OlympiadBench (He et al., 2024), the five benchmarks used by Liu et al. (2026)); knowledge (MMLU-Pro (Wang et al., 2024) and GPQA-Diamond (Rein et al., 2024)); logical reasoning (BBH Logical Deduction with three and five objects and Web of Lies (Suzgun et al., 2023)); and spatial and state tracking (BBH Tracking Shuffled Objects, Geometric Shapes, and Navigate). The headline number is the unweighted mean over the 13 benchmarks.

5.2 EMPIRICAL RESULTS

RQ1: Distillation from synthesised games. Table 1 compares the distillation settings on four models (per-benchmark results in Appendix D.2). We make two observations. First, the synthesised games are the strongest source of reasoning data on three of the four models. On Qwen3-4B-Base, GAMESMITH (matched) raises the 13-benchmark mean from 45.5 to 62.5, compared with 60.8 for Non-game, 60.6 for SPIRAL, and 28.8 for Format (Appendix D.3). Qwen3-8B-Base and GLM-4-9B-0414 exhibit the same ordering. On Mistral-Nemo-Instruct-2407, where game play transfers weakly, non-game reasoning data at the same token budget transfers better, by 5.8 points, and both game-based settings lose ground on GPQA-Diamond (Table 17). Note that the Non-game control is built from eight annotated datasets, keeps only traces that match the gold answer, and is 43% competition mathematics (Appendix C.1). In contrast, GAMESMITH uses no annotation of any kind, yet on Qwen3-4B-Base it still matches that corpus on logical reasoning (83.4 against 84.1) and outperforms it on mathematics (45.7 against 40.6), a capability that the games do not contain at all. The other two models on which game play transfers behave in the same way. Beyond needing no annotation, game data carries an engine-computed reward, so the same corpus drives the self-play stage of Table 2, where annotated data has no further use, and its supply grows on demand (RQ3). Second, compared with SPIRAL, the control that changes only which games the teacher plays, the synthesised games are worth more per token on every model, by between 1.9 and 5.2 points. Synthesised games are therefore the stronger source of game data on every model, and the stronger source of reasoning data on all but the weakest of them.

RQ2: Self-play on top of distillation. Table 2 reports three self-play pipelines: SPIRAL's three games with RAE from the SPIRAL distillation checkpoint, which is SPIRAL's original recipe, the synthesised corpus with RAE from the GAMESMITH checkpoint, and GAMESMITH, i.e., the same corpus and checkpoint with CRAB. The first two differ in both the checkpoint and the games and therefore compare complete pipelines. The last two share both and differ in the estimator (RAE vs. CRAB). CRAB improves on the distilled model and exceeds RAE on every model. On Qwen3-4B-Base, self-play with CRAB raises the mean from 62.5 to 64.9, whereas RAE on the same corpus and checkpoint reaches only 62.7 and the SPIRAL pipeline reaches 62.5 from 60.6. The other three models give the same ordering, and on Mistral-Nemo-Instruct-2407 and GLM-4-9B-0414 RAE falls below its starting point (47.9 to 47.3 and 65.1 to 64.9) while CRAB stays above it. The gain from self-play is smallest on GLM-4-9B-0414 (+0.3), where distillation already saturates the model at 65.1, so there is little left for self-play to add. RAE on the synthesised corpus is also unstable: after an early peak its scores fall well below the starting point for most of the budget, so its best checkpoint typically lies within the first 40 steps (Appendix D.5). A comparison of the two estimators with one

[1] https://huggingface.co/datasets/AI-MO/aimo-validation-amc

Table 1: Distillation results across models (pass@1 %, 8,192-token budget): capability-group means and the 13-benchmark mean. All SFT settings share the same teacher (Qwen3-32B), format, and token budget. Bold indicates the best value in each row. A shaded cell indicates that GAMESMITH exceeds the SPIRAL baseline on that row.

			Controls			GAMESMITH
Model	Capability	Base	Format	Non-game	SPIRAL	matched
Qwen3-4B-Base	Mathematics	32.5	10.7	40.6	39.6	**45.7**
	Knowledge	42.9	34.5	47.4	48.3	**49.6**
	Logical reasoning	54.9	50.9	84.1	**85.5**	83.4
	Spatial & tracking	59.5	33.1	**80.4**	78.8	78.4
	Average (13 benchmarks)	45.5	28.8	60.8	60.6	**62.5**
Qwen3-8B-Base	Mathematics	37.4	7.2	44.4	50.5	**51.6**
	Knowledge	48.5	4.3	55.4	56.9	**58.4**
	Logical reasoning	78.1	25.0	94.7	90.8	**95.4**
	Spatial & tracking	59.0	17.6	**85.6**	83.4	84.2
	Average (13 benchmarks)	53.5	13.3	67.2	68.4	**70.3**
Mistral-Nemo-Instruct-2407	Mathematics	16.1	2.1	**19.6**	12.3	17.2
	Knowledge	34.1	2.3	**41.2**	28.4	33.4
	Logical reasoning	70.0	14.5	**93.9**	76.5	80.3
	Spatial & tracking	66.9	16.9	**78.4**	69.0	76.2
	Average (13 benchmarks)	43.1	8.4	**53.7**	42.7	47.9
GLM-4-9B-0414	Mathematics	32.2	2.7	34.5	38.5	**40.3**
	Knowledge	48.1	12.4	48.1	48.2	**50.1**
	Logical reasoning	86.3	33.5	94.5	92.8	**95.0**
	Spatial & tracking	63.4	30.5	83.8	82.6	**86.4**
	Average (13 benchmarks)	54.3	17.7	61.8	62.7	**65.1**

Table 2: Self-play post-training results across models (13-benchmark mean pass@1 %).

		SPIRAL games		GAMESMITH games		
Model	Base	Distill.	+RL (RAE)	Distill.	+RL (RAE)	+RL (CRAB)
Qwen3-4B-Base	45.5	60.6	62.5	62.5	62.7	**64.9**
Qwen3-8B-Base	53.5	68.4	68.8	70.3	72.0	**73.1**
Mistral-Nemo-Instruct-2407	43.1	42.7	42.9	47.9	47.3	**48.8**
GLM-4-9B-0414	54.3	62.7	63.8	65.1	64.9	**65.4**

episode per variant is reported in Appendix D.4. Across models, the full GAMESMITH pipeline exceeds the full SPIRAL pipeline by 1.6 to 5.9 points, and CRAB exceeds RAE on the same corpus by 0.5 to 2.2 points (win rates on held-out game variants are reported in Appendix D.7).

RQ3: Scaling the number of families and the number of trajectories. A larger corpus can mean more game families or more trajectories, and Figure 3 separates the two on Qwen3-4B-Base: transfer increases with both. With the number of trajectories fixed, the mean increases from 59.1 at 4 families to 63.5 at 23, with the largest step between 4 and 8 families, and every capability group improves, with logical reasoning improving the most. With all 29 families, the mean rises steeply up to about 1,000 trajectories (57.0 $\rightarrow$ 62.3) and remains flat thereafter: 1,000 trajectories already exceed the SPIRAL performance, and the matched budget of Table 1 lies on the flat part of the curve, so the benefit comes from covering more games and is reached with few trajectories.

RQ4: Corpus diversity and which capabilities transfer. The corpus is more diverse than the three SPIRAL games and spans a wider range of game-tree complexity (Appendix D.1): the Vendi score by mechanic is 9.1 against 2.5, a rule change flips between 0.02 and 1.00 of outcomes, and game-tree complexity spans $[0.7, 68]$ across the 336 variants, supplied by the size variants.

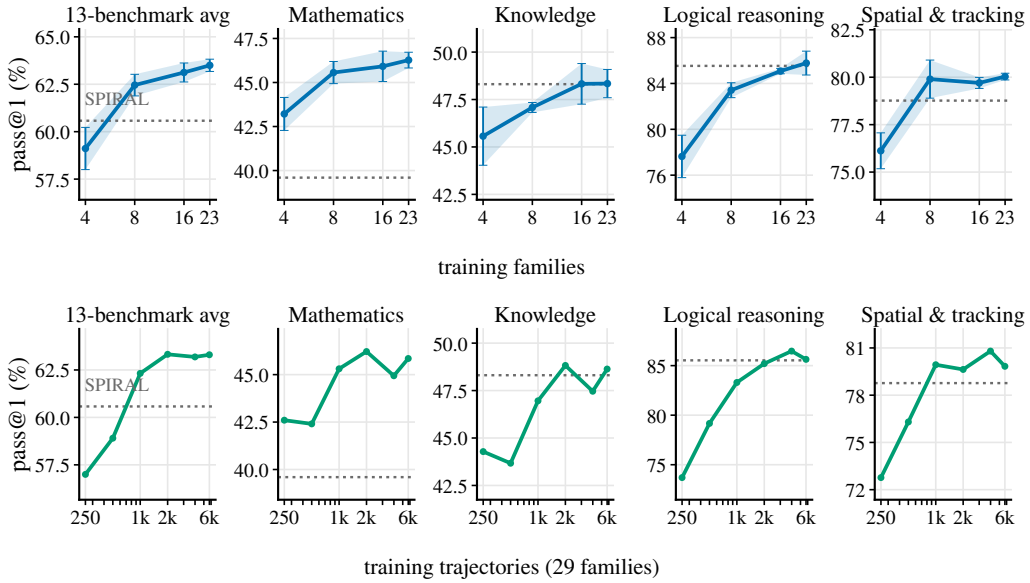

Figure 3: Distillation transfer by capability group on Qwen3-4B-Base (pass@1 %). **Top**: scaling the number of families ($4 \rightarrow 23$) at a fixed number of trajectories, showing the mean and one standard deviation over three draws of families. **Bottom**: scaling the number of trajectories with all 29 families. Dotted lines mark the SPIRAL performance.

When read by capability group, Tables 1 and 2 and Figure 3 agree on what game data teaches. Distillation improves most the two capabilities that the games exercise most: multi-step deduction over stated constraints (logical reasoning, $+28.5$ from Base) and tracking a state through a sequence of moves (spatial and state tracking, $+18.9$). Mathematics improves less ($+13.2$) and knowledge the least ($+6.7$). Self-play sharpens the same profile: the RL gain is concentrated on logical reasoning ($+6.5$ on Qwen3-4B-Base), where the deduction tasks most closely resemble the game decisions for which the policy is rewarded. The increment of the synthesised games over the SPIRAL games has a different profile: on Qwen3-4B-Base it is concentrated on mathematics ($+6.1$), with the two groups the games exercise most at or slightly below SPIRAL (-2.1 and -0.4), and on the other three models it is positive in every group (Table 1). What the synthesised games add over the seed games is therefore not confined to the capabilities that game data teaches best. Two features of the corpus account for this: the seed games already exercise deduction and state tracking, where the SPIRAL setting reaches 85.5 and 78.8 on Qwen3-4B-Base, so more games of the same kind add little, whereas the betting and negotiation families score hands and inventories by arithmetic (sums modulo M, bitwise XOR, target sums, set and tier bonuses, Table 7), so their teacher traces carry numerical computation that the seed games do not require.

6 Conclusion

We presented GameSmith, a framework for scaling LLM post-training with synthesised two-player zero-sum games. It combines constrained game synthesis and verification with distillation of teacher self-play and self-play reinforcement learning, and its advantage estimator, Crab, shares information across game variants where observations of individual variants are limited. Across four models and 13 reasoning benchmarks, distillation on the synthesised games outperforms distillation on the SPIRAL games under matched token budgets, self-play with Crab adds up to 2.8 points on top of distillation and exceeds both RAE on the same corpus and the SPIRAL pipeline on every model, and transfer improves as more game families are included, with a significant improvement already at $1{,}000$ trajectories. These findings support verified game synthesis as a scalable source of distillation data and reinforcement learning environments whose rewards come directly from game outcomes rather than from annotation.

REPRODUCIBILITY STATEMENT

The templates and their hook contracts are provided in Appendix A.1, the verification tests with their drivers, seeds, and relations in Appendix A.2, the admitted games and the variants used at each training stage in Appendix A.4.1 and A.4.2, the proof of Lemma 1 in Appendix B.1, the hyperparameters, software versions, hardware, and evaluation protocol in Appendices C.2 and C.4, the licences of every asset in Appendix C.5, the per-benchmark results in Appendix D.2, and the verbatim prompts of the synthesis pipeline in Appendix E. The corpus, the synthesis and verification code, the training configurations, and the evaluation harness will be released upon acceptance.

AI USE STATEMENT

In this work, we used generative AI tools to generate synthetic data sets and to implement methods: GPT-5 writes the game specifications and their implementations (§4.1), Qwen3-32B writes the independent re-implementations and the self-play traces from which the models are distilled (§4.2), and an LLM runs the playtest (Appendix A.2). We have not used generative AI tools to help develop theoretical models or conceptual frameworks, formulate mathematical claims, provide critical ingredients for proving mathematical claims, assist in the writing of proofs, propose or refine hypotheses, design or provide feedback on research methodology or experiments, clean and reformat datasets, or interpret results, and assisting with translation and supporting qualitative and thematic data analysis are not applicable to this work. Additionally, we used generative AI tools for the creation of artifacts, namely the synthesised game corpus, and an LLM assistant (Claude) to create or edit software code and to edit the paper to improve readability. We have reviewed all AI-assisted work: every generated game is verified by the replay tests and the independent re-implementation before use, every teacher trace of the non-game control is checked against its gold answer, and the AI-assisted code and text were checked by the authors. We take responsibility for the final content of this work, including text, claims or artifacts produced with the aid of generative AI.

REFERENCES

Arash Ahmadian, Chris Cremer, Matthias Gallé, Marzieh Fadaee, Julia Kreutzer, Olivier Pietquin, Ahmet Üstün, and Sara Hooker. Back to basics: Revisiting REINFORCE-style optimization for learning from human feedback in LLMs. In Lun-Wei Ku, Andre Martins, and Vivek Srikumar (eds.), *Proceedings of the 62nd Annual Meeting of the Association for Computational Linguistics (Volume 1: Long Papers)*, pp. 12248–12267, Bangkok, Thailand, August 2024. Association for Computational Linguistics. doi: 10.18653/v1/2024.acl-long.662. URL https://aclanthology.org/2024.acl-long.662/.

L.V. Allis. *Searching for solutions in games and artificial intelligence*. PhD thesis, Maastricht University, January 1994.

Bowen Baker, Ingmar Kanitscheider, Todor Markov, Yi Wu, Glenn Powell, Bob McGrew, and Igor Mordatch. Emergent tool use from multi-agent autocurricula. In *International Conference on Learning Representations*, 2020. URL https://openreview.net/forum?id=SkxpxJBKwS.

Peter L. Bartlett and Shahar Mendelson. Rademacher and gaussian complexities: risk bounds and structural results. *J. Mach. Learn. Res.*, 3(null):463–482, March 2003. ISSN 1532-4435.

Federico Bianchi, Patrick John Chia, Mert Yuksekgonul, Jacopo Tagliabue, Dan Jurafsky, and James Zou. How well can llms negotiate? negotiationarena platform and analysis. In *Proceedings of the 41st International Conference on Machine Learning*, ICML'24. JMLR.org, 2024.

Jiaqi Chen, Bang Zhang, Ruotian Ma, Peisong Wang, Xiaodan Liang, Zhaopeng Tu, Xiaolong Li, and Kwan-Yee K. Wong. SPC: Evolving self-play critic via adversarial games for LLM reasoning. In *The Thirty-ninth Annual Conference on Neural Information Processing Systems*, 2025a. URL https://openreview.net/forum?id=JddJvNSiHk.

Lili Chen, Mihir Prabhudesai, Katerina Fragkiadaki, Hao Liu, and Deepak Pathak. Self-questioning language models, 2025b. URL https://arxiv.org/abs/2508.03682.

Shuxiao Chen, Edgar Dobriban, and Jane H. Lee. A group-theoretic framework for data augmentation. *Journal of Machine Learning Research*, 21(245):1–71, 2020. URL http://jmlr.org/papers/v21/20-163.html.

Pengyu Cheng, Tianhao Hu, Han Xu, Zhisong Zhang, Yong Dai, Lei Han, nan du, and Xiaolong Li. Self-playing adversarial language game enhances LLM reasoning. In *The Thirty-eighth Annual Conference on Neural Information Processing Systems*, 2024. URL https://openreview.net/forum?id=oCGkSH7ys2.

Karl Cobbe, Oleg Klimov, Chris Hesse, Taehoon Kim, and John Schulman. Quantifying generalization in reinforcement learning. In Kamalika Chaudhuri and Ruslan Salakhutdinov (eds.), *Proceedings of the 36th International Conference on Machine Learning*, volume 97 of *Proceedings of Machine Learning Research*, pp. 1282–1289. PMLR, 09–15 Jun 2019. URL https://proceedings.mlr.press/v97/cobbe19a.html.

Anthony Costarelli, Mat Allen, Roman Hauksson, Grace Sodunke, Suhas Hariharan, Carlson Cheng, Wenjie Li, Joshua Clymer, and Arjun Yadav. Gamebench: Evaluating strategic reasoning abilities of llm agents, 2024. URL https://arxiv.org/abs/2406.06613.

DeepSeek-AI. Deepseek-r1 incentivizes reasoning in llms through reinforcement learning. *Nature*, 645(8081):633–638, September 2025. ISSN 1476-4687. doi: 10.1038/s41586-025-09422-z. URL http://dx.doi.org/10.1038/s41586-025-09422-z.

Michael Dennis, Natasha Jaques, Eugene Vinitsky, Alexandre Bayen, Stuart Russell, Andrew Critch, and Sergey Levine. Emergent complexity and zero-shot transfer via unsupervised environment design. In *Proceedings of the 34th International Conference on Neural Information Processing Systems*, NIPS '20, Red Hook, NY, USA, 2020. Curran Associates Inc. ISBN 9781713829546.

Guanting Dong, Junting Lu, Junjie Huang, Wanjun Zhong, Longxiang Liu, Shijue Huang, Zhenyu Li, Yang Zhao, Xiaoshuai Song, Xiaoxi Li, Jiajie Jin, Yutao Zhu, Hanbin Wang, Fangyu Lei, Qinyu Luo, Mingyang Chen, Zehui Chen, Jiazhan Feng, Ji-Rong Wen, and Zhicheng Dou. Agent-world: Scaling real-world environment synthesis for evolving general agent intelligence, 2026. URL https://arxiv.org/abs/2604.18292.

Jinhao Duan, Renming Zhang, James Diffenderfer, Bhavya Kailkhura, Lichao Sun, Elias Stengel-Eskin, Mohit Bansal, Tianlong Chen, and Kaidi Xu. Gtbench: uncovering the strategic reasoning limitations of llms via game-theoretic evaluations. In *Proceedings of the 38th International Conference on Neural Information Processing Systems*, NIPS '24, Red Hook, NY, USA, 2024. Curran Associates Inc. ISBN 9798331314385.

Bryn Elesedy and Sheheryar Zaidi. Provably strict generalisation benefit for equivariant models. In Marina Meila and Tong Zhang (eds.), *Proceedings of the 38th International Conference on Machine Learning*, volume 139 of *Proceedings of Machine Learning Research*, pp. 2959–2969. PMLR, 18–24 Jul 2021. URL https://proceedings.mlr.press/v139/elesedy21a.html.

Maxence Faldor, Jenny Zhang, Antoine Cully, and Jeff Clune. OMNI-EPIC: Open-endedness via models of human notions of interestingness with environments programmed in code. In *The Thirteenth International Conference on Learning Representations*, 2025. URL https://openreview.net/forum?id=Y1XkzMJpPd.

Team GLM. Chatglm: A family of large language models from glm-130b to glm-4 all tools, 2024. URL https://arxiv.org/abs/2406.12793.

Leon Guertler, Bobby Cheng, Simon Yu, Bo Liu, Leshem Choshen, and Cheston Tan. Textarena, 2025. URL https://arxiv.org/abs/2504.11442.

Chaoqun He, Renjie Luo, Yuzhuo Bai, Shengding Hu, Zhen Thai, Junhao Shen, Jinyi Hu, Xu Han, Yujie Huang, Yuxiang Zhang, Jie Liu, Lei Qi, Zhiyuan Liu, and Maosong Sun. OlympiadBench: A challenging benchmark for promoting AGI with olympiad-level bilingual multimodal scientific problems. In Lun-Wei Ku, Andre Martins, and Vivek Srikumar (eds.), *Proceedings of the*

62nd Annual Meeting of the Association for Computational Linguistics (Volume 1: Long Papers), pp. 3828–3850, Bangkok, Thailand, August 2024. Association for Computational Linguistics. doi: 10.18653/v1/2024.acl-long.211. URL https://aclanthology.org/2024.acl-long.211/.

Dan Hendrycks, Collin Burns, Saurav Kadavath, Akul Arora, Steven Basart, Eric Tang, Dawn Song, and Jacob Steinhardt. Measuring mathematical problem solving with the math dataset. In J. Vanschoren and S. Yeung (eds.), *Proceedings of the Neural Information Processing Systems Track on Datasets and Benchmarks*, volume 1, 2021. URL https://datasets-benchmarks-proceedings.neurips.cc/paper_files/paper/2021/file/be83ab3ecd0db773eb2dc1b0a17836a1-Paper-round2.pdf.

Chengsong Huang, Wenhao Yu, Xiaoyang Wang, Hongming Zhang, Zongxia Li, Ruosen Li, Jiaxin Huang, Haitao Mi, and Dong Yu. R-zero: Self-evolving reasoning LLM from zero data. In *The Fourteenth International Conference on Learning Representations*, 2026. URL https://openreview.net/forum?id=96apU6YzSO.

Chaobo Jia, Ruipeng Wan, Ting Sun, Weihao Tan, Borui Wan, Yuxuan Tong, Guangming Sheng, and Hong Xu. Gamegen-verifier: Parallel keypoint-based verification for llm-generated games via runtime state injection, 2026. URL https://arxiv.org/abs/2605.07442.

Amirhossein Kazemnejad, Milad Aghajohari, Eva Portelance, Alessandro Sordoni, Siva Reddy, Aaron Courville, and Nicolas Le Roux. VinePPO: Refining credit assignment in RL training of LLMs. In *Forty-second International Conference on Machine Learning*, 2025. URL https://openreview.net/forum?id=Myx2kJFzAn.

Jakub Grudzien Kuba, Mengting Gu, Qi Ma, Yuandong Tian, Vijai Mohan, and Jason Chen. Language self-play for data-free training, 2025. URL https://arxiv.org/abs/2509.07414.

Aitor Lewkowycz, Anders Andreassen, David Dohan, Ethan Dyer, Henryk Michalewski, Vinay Ramasesh, Ambrose Slone, Cem Anil, Imanol Schlag, Theo Gutman-Solo, Yuhuai Wu, Behnam Neyshabur, Guy Gur-Ari, and Vedant Misra. Solving quantitative reasoning problems with language models. In *Proceedings of the 36th International Conference on Neural Information Processing Systems*, NIPS '22, Red Hook, NY, USA, 2022. Curran Associates Inc. ISBN 9781713871088.

Weixian Waylon Li, Yftah Ziser, Maximin Coavoux, and Shay B. Cohen. BERT is not the count: Learning to match mathematical statements with proofs. In Andreas Vlachos and Isabelle Augenstein (eds.), *Proceedings of the 17th Conference of the European Chapter of the Association for Computational Linguistics*, pp. 3581–3593, Dubrovnik, Croatia, May 2023. Association for Computational Linguistics. doi: 10.18653/v1/2023.eacl-main.260. URL https://aclanthology.org/2023.eacl-main.260/.

Weixian Waylon Li, Yuchen Niu, Yongxin Yang, Keshuang Li, Tiejun Ma, and Shay B Cohen. Spectral attention steering for prompt highlighting. In C. Vondrick, B. Hariharan, C. Raffel, L. Pinto, D. Yang, and A. Faust (eds.), *International Conference on Learning Representations*, volume 2026, pp. 29891–29917, 2026a. URL https://proceedings.iclr.cc/paper_files/paper/2026/file/32ddf8ee55540539eb46083cd72361e8-Paper-Conference.pdf.

Weixian Waylon Li, Jiaxin Zhang, Xianan Jim Yang, Tiejun Ma, and Yiwen Guo. Time is not a label: Continuous phase rotation for temporal knowledge graphs and agentic memory, 2026b. URL https://arxiv.org/abs/2604.11544.

Hunter Lightman, Vineet Kosaraju, Yuri Burda, Harrison Edwards, Bowen Baker, Teddy Lee, Jan Leike, John Schulman, Ilya Sutskever, and Karl Cobbe. Let's verify step by step. In *The Twelfth International Conference on Learning Representations*, 2024. URL https://openreview.net/forum?id=v8L0pN6EOi.

Bo Liu, Chuanyang Jin, Seungone Kim, Weizhe Yuan, Wenting Zhao, Ilia Kulikov, Xian Li, Sainbayar Sukhbaatar, Jack Lanchantin, and Jason Weston. Spice: Self-play in corpus environments improves reasoning, 2025a. URL https://arxiv.org/abs/2510.24684.

Bo Liu, Simon Yu, Zichen Liu, Leon Guertler, Penghui Qi, Daniel Balcells, Mickel Liu, Cheston Tan, Weiyan Shi, Min Lin, Wee Sun Lee, and Natasha Jaques. SPIRAL: Self-play on zero-sum games incentivizes reasoning via multi-agent multi-turn reinforcement learning. In *The Fourteenth International Conference on Learning Representations*, 2026. URL https://openreview.net/forum?id=7Yayy5fNLg.

Zichen Liu, Changyu Chen, Wenjun Li, Penghui Qi, Tianyu Pang, Chao Du, Wee Sun Lee, and Min Lin. Understanding r1-zero-like training: A critical perspective. In *Second Conference on Language Modeling*, 2025b. URL https://openreview.net/forum?id=5PAF7PAY2Y.

Michael Matthews, Michael Beukman, Chris Lu, and Jakob Nicolaus Foerster. Kinetix: Investigating the training of general agents through open-ended physics-based control tasks. In *The Thirteenth International Conference on Learning Representations*, 2025. URL https://openreview.net/forum?id=zCxGCdzreM.

Long Ouyang, Jeff Wu, Xu Jiang, Diogo Almeida, Carroll L. Wainwright, Pamela Mishkin, Chong Zhang, Sandhini Agarwal, Katarina Slama, Alex Ray, John Schulman, Jacob Hilton, Fraser Kelton, Luke Miller, Maddie Simens, Amanda Askell, Peter Welinder, Paul Christiano, Jan Leike, and Ryan Lowe. Training language models to follow instructions with human feedback. In *Proceedings of the 36th International Conference on Neural Information Processing Systems*, NIPS '22, Red Hook, NY, USA, 2022. Curran Associates Inc. ISBN 9781713871088.

Tian Qin, Fengxiang He, Dingfeng Shi, Wenbing Huang, and Dacheng Tao. Benefits of permutation-equivariance in auction mechanisms. In *Proceedings of the 36th International Conference on Neural Information Processing Systems*, NIPS '22, Red Hook, NY, USA, 2022. Curran Associates Inc. ISBN 9781713871088.

David Rein, Betty Li Hou, Asa Cooper Stickland, Jackson Petty, Richard Yuanzhe Pang, Julien Dirani, Julian Michael, and Samuel R. Bowman. GPQA: A graduate-level google-proof q&a benchmark. In *First Conference on Language Modeling*, 2024. URL https://openreview.net/forum?id=Ti67584b98.

John Schulman, Filip Wolski, Prafulla Dhariwal, Alec Radford, and Oleg Klimov. Proximal policy optimization algorithms, 2017. URL https://arxiv.org/abs/1707.06347.

Sheikh Shafayat, Fahim Tajwar, Ruslan Salakhutdinov, Jeff Schneider, and Andrea Zanette. Can large reasoning models self-train?, 2025. URL https://arxiv.org/abs/2505.21444.

Zhihong Shao, Peiyi Wang, Qihao Zhu, Runxin Xu, Junxiao Song, Xiao Bi, Haowei Zhang, Mingchuan Zhang, Y. K. Li, Y. Wu, and Daya Guo. Deepseekmath: Pushing the limits of mathematical reasoning in open language models, 2024. URL https://arxiv.org/abs/2402.03300.

Yucheng Shi, Zhenwen Liang, Kishan Panaganti, Dian Yu, Wenhao Yu, and Haitao Mi. Learning to build the environment: Self-evolving reasoning rl via verifiable environment synthesis, 2026. URL https://arxiv.org/abs/2605.14392.

David Silver, Aja Huang, Christopher Maddison, Arthur Guez, Laurent Sifre, George Driessche, Julian Schrittwieser, Ioannis Antonoglou, Veda Panneershelvam, Marc Lanctot, Sander Dieleman, Dominik Grewe, John Nham, Nal Kalchbrenner, Ilya Sutskever, Timothy Lillicrap, Madeleine Leach, Koray Kavukcuoglu, Thore Graepel, and Demis Hassabis. Mastering the game of go with deep neural networks and tree search. *Nature*, 529:484–489, 01 2016. doi: 10.1038/nature16961.

David Silver, Thomas Hubert, Julian Schrittwieser, Ioannis Antonoglou, Matthew Lai, Arthur Guez, Marc Lanctot, Laurent Sifre, Dharshan Kumaran, Thore Graepel, Timothy Lillicrap, Karen Simonyan, and Demis Hassabis. A general reinforcement learning algorithm that masters chess, shogi, and go through self-play. *Science*, 362(6419):1140–1144, 2018. doi: 10.1126/science.aar6404. URL https://www.science.org/doi/abs/10.1126/science.aar6404.

Avi Singh, John D Co-Reyes, Rishabh Agarwal, Ankesh Anand, Piyush Patil, Xavier Garcia, Peter J Liu, James Harrison, Jaehoon Lee, Kelvin Xu, Aaron T Parisi, Abhishek Kumar, Alexander A

Alemi, Alex Rizkowsky, Azade Nova, Ben Adlam, Bernd Bohnet, Gamaleldin Fathy Elsayed, Hanie Sedghi, Igor Mordatch, Isabelle Simpson, Izzeddin Gur, Jasper Snoek, Jeffrey Pennington, Jiri Hron, Kathleen Kenealy, Kevin Swersky, Kshiteej Mahajan, Laura A Culp, Lechao Xiao, Maxwell Bileschi, Noah Constant, Roman Novak, Rosanne Liu, Tris Warkentin, Yamini Bansal, Ethan Dyer, Behnam Neyshabur, Jascha Sohl-Dickstein, and Noah Fiedel. Beyond human data: Scaling self-training for problem-solving with language models. *Transactions on Machine Learning Research*, 2024. ISSN 2835-8856. URL https://openreview.net/forum?id=lNAyUngGFK. Expert Certification.

Xiaoshuai Song, Haofei Chang, Guanting Dong, Yutao Zhu, Ji-Rong Wen, and Zhicheng Dou. EnvScaler: Scaling tool-interactive environments for LLM agent via programmatic synthesis. In Maria Liakata, Viviane P. Moreira, Jiajun Zhang, and David Jurgens (eds.), *Findings of the Association for Computational Linguistics: ACL 2026*, pp. 8326–8357, San Diego, California, United States, July 2026. Association for Computational Linguistics. ISBN 979-8-89176-395-1. doi: 10.18653/v1/2026.findings-acl.407. URL https://aclanthology.org/2026.findings-acl.407/.

Zafir Stojanovski, Oliver Stanley, Joe Sharratt, Richard Jones, Abdulhakeem Adefioye, Jean Kaddour, and Andreas Köpf. Reasoning gym: Reasoning environments for reinforcement learning with verifiable rewards. In *The Thirty-ninth Annual Conference on Neural Information Processing Systems Datasets and Benchmarks Track*, 2026. URL https://openreview.net/forum?id=GqYSunGmp7.

Haoxiang Sun, Yingqian Min, Zhipeng Chen, Xin Zhao, and Ji-Rong Wen. Challenging the boundaries of reasoning: An olympiad-level math benchmark for large language models. In Maria Liakata, Viviane P. Moreira, Jiajun Zhang, and David Jurgens (eds.), *Proceedings of the 64th Annual Meeting of the Association for Computational Linguistics (Volume 1: Long Papers)*, pp. 17438–17457, San Diego, California, United States, July 2026. Association for Computational Linguistics. ISBN 979-8-89176-390-6. doi: 10.18653/v1/2026.acl-long.792. URL https://aclanthology.org/2026.acl-long.792/.

Mirac Suzgun, Nathan Scales, Nathanael Schärli, Sebastian Gehrmann, Yi Tay, Hyung Won Chung, Aakanksha Chowdhery, Quoc Le, Ed Chi, Denny Zhou, and Jason Wei. Challenging BIG-bench tasks and whether chain-of-thought can solve them. In Anna Rogers, Jordan Boyd-Graber, and Naoaki Okazaki (eds.), *Findings of the Association for Computational Linguistics: ACL 2023*, pp. 13003–13051, Toronto, Canada, July 2023. Association for Computational Linguistics. doi: 10.18653/v1/2023.findings-acl.824. URL https://aclanthology.org/2023.findings-acl.824/.

Josh Tobin, Rachel Fong, Alex Ray, Jonas Schneider, Wojciech Zaremba, and Pieter Abbeel. Domain randomization for transferring deep neural networks from simulation to the real world. In *2017 IEEE/RSJ International Conference on Intelligent Robots and Systems (IROS)*, pp. 23–30. IEEE Press, 2017. doi: 10.1109/IROS.2017.8202133. URL https://doi.org/10.1109/IROS.2017.8202133.

Finn van der Knaap, Kejiang Qian, Zheng Xu, and Fengxiang He. Prism: Parallel reward integration with symmetry for morl, 2026. URL https://arxiv.org/abs/2602.18277.

Vivek Verma, David Huang, William Chen, Dan Klein, and Nicholas Tomlin. Measuring general intelligence with generated games, 2025. URL https://arxiv.org/abs/2505.07215.

Rui Wang, Joel Lehman, Jeff Clune, and Kenneth O. Stanley. Paired open-ended trailblazer (poet): Endlessly generating increasingly complex and diverse learning environments and their solutions, 2019. URL https://arxiv.org/abs/1901.01753.

Yubo Wang, Xueguang Ma, Ge Zhang, Yuansheng Ni, Abhranil Chandra, Shiguang Guo, Weiming Ren, Aaran Arulraj, Xuan He, Ziyan Jiang, Tianle Li, Max Ku, Kai Wang, Alex Zhuang, Rongqi Fan, Xiang Yue, and Wenhu Chen. Mmlu-pro: a more robust and challenging multi-task language understanding benchmark. In *Proceedings of the 38th International Conference on Neural Information Processing Systems*, NIPS '24, Red Hook, NY, USA, 2024. Curran Associates Inc. ISBN 9798331314385.

Zhaoyang Wang, Canwen Xu, Boyi Liu, Yite Wang, Siwei Han, Zhewei Yao, Huaxiu Yao, and Yuxiong He. Agent world model: Infinity synthetic environments for agentic reinforcement learning. In *Forty-third International Conference on Machine Learning*, 2026. URL https://openreview.net/forum?id=OvLnVkV14P.

An Yang, Anfeng Li, Baosong Yang, Beichen Zhang, Binyuan Hui, Bo Zheng, Bowen Yu, Chang Gao, Chengen Huang, Chenxu Lv, Chujie Zheng, Dayiheng Liu, Fan Zhou, Fei Huang, Feng Hu, Hao Ge, Haoran Wei, Huan Lin, Jialong Tang, Jian Yang, Jianhong Tu, Jianwei Zhang, Jianxin Yang, Jiaxi Yang, Jing Zhou, Jingren Zhou, Junyang Lin, Kai Dang, Keqin Bao, Kexin Yang, Le Yu, Lianghao Deng, Mei Li, Mingfeng Xue, Mingze Li, Pei Zhang, Peng Wang, Qin Zhu, Rui Men, Ruize Gao, Shixuan Liu, Shuang Luo, Tianhao Li, Tianyi Tang, Wenbiao Yin, Xingzhang Ren, Xinyu Wang, Xinyu Zhang, Xuancheng Ren, Yang Fan, Yang Su, Yichang Zhang, Yinger Zhang, Yu Wan, Yuqiong Liu, Zekun Wang, Zeyu Cui, Zhenru Zhang, Zhipeng Zhou, and Zihan Qiu. Qwen3 technical report, 2025. URL https://arxiv.org/abs/2505.09388.

Qiying Yu, Zheng Zhang, Ruofei Zhu, Yufeng Yuan, Xiaochen Zuo, YuYue, Weinan Dai, Tiantian Fan, Gaohong Liu, Juncai Liu, LingJun Liu, Xin Liu, Haibin Lin, Zhiqi Lin, Bole Ma, Guangming Sheng, Yuxuan Tong, Chi Zhang, Mofan Zhang, Ru Zhang, Wang Zhang, Hang Zhu, Jinhua Zhu, Jiaze Chen, Jiangjie Chen, Chengyi Wang, Hongli Yu, Yuxuan Song, Xiangpeng Wei, Hao Zhou, Jingjing Liu, Wei-Ying Ma, Ya-Qin Zhang, Lin Yan, Yonghui Wu, and Mingxuan Wang. DAPO: An open-source LLM reinforcement learning system at scale. In *The Thirty-ninth Annual Conference on Neural Information Processing Systems*, 2025. URL https://openreview.net/forum?id=2a36EMSSTp.

Huining Yuan, Zelai Xu, Zheyue Tan, Xiangmin Yi, Mo Guang, Kaiwen Long, Haojia Hui, Boxun Li, Xinlei Chen, Bo Zhao, Xiao-Ping Zhang, Chao Yu, and Yu Wang. MARSHAL: Incentivizing multi-agent reasoning via self-play with strategic LLMs. In *The Fourteenth International Conference on Learning Representations*, 2026. URL https://openreview.net/forum?id=GCd5v3ehmr.

Weizhe Yuan, Richard Yuanzhe Pang, Kyunghyun Cho, Xian Li, Sainbayar Sukhbaatar, Jing Xu, and Jason Weston. Self-rewarding language models. In *Proceedings of the 41st International Conference on Machine Learning*, ICML'24. JMLR.org, 2024.

Eric Zelikman, Yuhuai Wu, Jesse Mu, and Noah Goodman. STar: Bootstrapping reasoning with reasoning. In Alice H. Oh, Alekh Agarwal, Danielle Belgrave, and Kyunghyun Cho (eds.), *Advances in Neural Information Processing Systems*, 2022. URL https://openreview.net/forum?id=_3ELRdg2sgI.

Zhiyuan Zeng, Hamish Ivison, Yiping Wang, Lifan Yuan, Shuyue Stella Li, Zhuorui Ye, Siting Li, Jacqueline He, Runlong Zhou, Tong Chen, Chenyang Zhao, Yulia Tsvetkov, Simon Shaolei Du, Natasha Jaques, Hao Peng, Pang Wei Koh, and Hannaneh Hajishirzi. RLVE: Scaling up reinforcement learning for language models with adaptive verifiable environments. In *Forty-third International Conference on Machine Learning*, 2026. URL https://openreview.net/forum?id=DRqjMnDQGq.

Andrew Zhao, Yiran Wu, Yang Yue, Tong Wu, Quentin Xu, Yang Yue, Matthieu Lin, Shenzhi Wang, Qingyun Wu, Zilong Zheng, and Gao Huang. Absolute zero: Reinforced self-play reasoning with zero data. In *The Thirty-ninth Annual Conference on Neural Information Processing Systems*, 2025. URL https://openreview.net/forum?id=neZSGqhxDa.

Chenyu Zhou, Qiliang Jiang, Shuning Wu, and Xu Zhou. The verifier is the curriculum: Precision sets the return on search in code self-distillation, 2026. URL https://arxiv.org/abs/2607.09709.

Ding-Xuan Zhou. The covering number in learning theory. *J. Complex.*, 18(3):739–767, September 2002. ISSN 0885-064X. doi: 10.1006/jcom.2002.0635. URL https://doi.org/10.1006/jcom.2002.0635.

Yifei Zhou, Sergey Levine, Jason E Weston, Xian Li, and Sainbayar Sukhbaatar. Self-challenging language model agents. In *The Thirty-ninth Annual Conference on Neural Information Processing Systems*, 2025. URL https://openreview.net/forum?id=9yusqX9DpR.

A ADDITIONAL DETAILS OF THE METHOD

A.1 TEMPLATE HOOKS AND STATE VALUES

Table 3 lists, for each template of the main study, the functions that the engineer must or may implement and what each of them returns. Everything else is part of the kernel, including dealing and hidden-state routing, the betting or offer state machine, board rendering, action parsing, the encoding e, reward assignment, and episode termination. Hooks receive canonical indices (player ids 0 and 1, canonical coordinates, rank indices, and resource indices) rather than display symbols, and they must be deterministic and free of I/O. The rules text is the only hook that produces text for the player, and it must describe the game through a dictionary of the current display labels, so that a change of encoding changes the text consistently. The state value $V(s)$ of §4.2 is computed by the kernel from these hooks and uses only information visible to the seat being valued, never the opponent's hidden state. For grid placement, it is the minimax outcome when the position is decided within two plies, and otherwise the mean outcome of 16 random playouts whose seed is derived from the position, so that V is a deterministic function of the state. For betting with a showdown, it combines the probability that the seat's own hand beats a random opponent hand drawn from the remaining deck, computed by exact enumeration and mapped to $[-1, 1]$, with the settled chip lead normalised by the largest possible chip total, weighted by the fraction of rounds remaining. For resource negotiation, it is the gain of the seat's own inventory score over its initial value under the seat's private valuation, normalised by the scale of a single trade.

Table 3: Engineer hooks per template. Each template also exposes a state value $V(s)$ (§4.2) computed by the kernel from these hooks.

Template	Hook and signature	Contract
Grid placement	`legal_moves(board, pid, extras)` → list of cells	optional, default is every empty cell
	`apply_move(board, pid, r, c, extras)`	optional, default writes `pid` into the cell
	`outcome(board, pid, r, c, extras)`	called after each placement, returns none, a win or loss for a player, or a draw
	`rules_text(cfg, player_id, symbols)` → str	rules in natural language using the two current symbols
	`init_extras()` → dict	optional per-episode state
Betting with showdown	`hand_value(hand, cfg)` → comparable	strength of a hand of rank indices, where the higher hand wins the showdown and equal values split the pot
	`rules_text(cfg, player_id, labels)` → str	rules using the current action words and rank labels
Resource negotiation	`inventory_score(quantities, values, cfg)` → int	score of an inventory under the player's private unit values, default $\sum_i q_i v_i$
	`menu(cfg)` → list of swaps	optional, the proposable trades as (give, get, give quantity, get quantity) in a stable order, default every ordered pair at base-value parity
	`trade_ok(give, get, gq, rq, quantities, cfg)` → bool	optional, default requires the proposer to hold the quantity given
	`rules_text(cfg, player_id, labels)` → str	rules using the current resource names, base values, and action words

A.2 DEFINITION OF THE VERIFICATION TESTS

Every replay test of §4.1 is a predicate of the same form. Formally, let $\rho(E, s, a_{1:t})$ denote the trajectory of environment E started from seed s under the action sequence $a_{1:t}$. A test c specifies which two environments to replay, a driver D_c, and a relation R_c that the two trajectories must satisfy on every seed of a fixed set $\mathcal{S}$:

$$c(g) \;\equiv\; \forall\, s \in \mathcal{S},\; \forall\, a_{1:t} \sim D_c :\; R_c\big(\rho(E_1, s, a_{1:t}),\, \rho(E_2, s, a_{1:t})\big). \tag{6}$$

Table 4 lists the replay tests in this form, together with the driver, the number of seeds, and the relation checked, followed by the agreement check against the independent re-implementation and the duplicate check.

Table 4: Replay tests, agreement check, and duplicate check as implemented. Each row is a predicate of the form of equation 6.

Test	Seeds	What is replayed, and what must hold on every seed	Property established
Encoding	40	Random legal actions in E_ϕ, mapped through e into an encoding variant $E_{\phi'}$. The sets of available actions must correspond under e at every step, and the final rewards must be identical.	hooks do not depend on the encoding
Rule	60	The same random action sequence in E_ϕ and in its rule variant. For an outcome-reversing rule every decisive outcome must be swapped, otherwise some outcome must differ, and for a legality rule the first-turn set of legal actions must differ.	the rule change is effective
Outcome	60 / 20 / 1	One variant under random play, a driver that submits illegal actions, and every rendered action label of the first turn. The two rewards must sum to zero and the episode must terminate, an illegal action must be penalised at once without stopping the engine, and every label must be accepted.	rewards are zero-sum and follow the hook verdict, termination, non-degeneracy
Information hiding	20	The same action sequence in E_ϕ and in a copy with the opponent's hidden cards, code, or private unit values replaced. The observation stream of the first player must be identical up to the showdown or reveal.	hooks do not leak hidden state
Playability	40	One variant with each seat driven by a reference bot maximising its own score. The bot must use the game's core action (for negotiation, at least 0.5 executed trades per episode) and at least 25% of episodes must be decisive.	the game can be played
Agreement (Agree)	60	The same labelled action sequence in g and in $\tilde{g}$. The final rewards must be identical.	the two implementations agree on every replayed outcome
Duplicate (Dup)	60	The same action sequence in g and in a fingerprint-close admitted game. The game is rejected if the outcomes match on every seed.	the game is new

Both the duplicate check and the degeneracy flag rely on a fingerprint of random play. Each game is fingerprinted from 80 episodes of random play by its mean episode length, mean branching factor, fraction of decisive outcomes, first-mover win share, and, for grid games, the fraction of the board filled. Two games on the same template whose fingerprints are close (episode length within 2, decisive fraction within 0.1, and fill fraction within 0.1) are replayed against each other from 60 shared seeds, and the later one is rejected if the outcomes match on every seed. The same fingerprint flags a game as degenerate, and thereby excludes it from training, if it produces only draws, if the first-mover win share lies outside $[0.1, 0.9]$, or if a grid game ends in fewer than four moves on average.

The independent re-implementation of each specification is written by a locally served Qwen3-32B, which belongs to a different model family from the GPT-5 generator, at temperature 0.6 with up to $10{,}000$ completion tokens and at most three attempts. It is prompted with the engineer system prompt of the same template and receives the template source, the specification, and the configuration defaults of the first implementation, but never the first implementation itself. Before the agreement check, the re-implementation must itself pass the outcome test of Table 4.

In the LLM playtest, a model plays one seat from the rules text and the current observation alone, and states with each move whether the game ends for it according to the rules. Its scores are the fraction of legal moves, the win rate against a random opponent, and the precision of those end-of-game claims against the engine. These scores are recorded as a diagnostic, a family whose legality score is below 0.7 is flagged, and no score plays a role in admission. The prompt is given in Appendix E.

The replay tests are calibrated on the three SPIRAL games. Each game is first run through the tests unmodified, and every test must pass. Known defects, including a reversed outcome and a corrupted action label, are then injected into its hooks, and the tests are run again.

One failure mode passed the first four tests and motivated the playability test. A negotiation family whose inventory score is strongly non-linear passes the outcome and information-hiding tests, and its random-play fingerprint is unremarkable, because random players do trade. Under a score-maximising reference bot, however, every swap on the default parity menu loses value for at least one side, so the bot never trades and every game ends in a draw. This failure mode is the reason why the engineer prompt for this template asks for a menu that is at parity under the game's own scoring rule.

A.3 Effectiveness of the verification tests

Table 4 lists the tests. In this subsection, we report what they did during synthesis and what they can be shown to catch. Specifically, we report three things: the candidates that each test eliminated during synthesis, the defects that each test catches when known defects are injected into the three seed games, and whether either result depends on the fixed seeds of Table 4.

What each test eliminated. Table 5 aggregates the admission logs of every synthesis run. The designer proposed 80 games, of which 76 were implemented within the attempt budget and 75 passed the replay tests, at 1.74 engineer attempts per game (Appendix A.4.1). Four of the seven tests rejected no candidate in this batch. Since a test that never fires provides no evidence of its own efficacy, this motivates the injection experiment below. Across the 613 certificate records stored with the corpus, none records a failure: every rejection that did occur is recorded separately, as a rejection record, a disagreement record, or a run report.

Injected defects. Because most tests were never triggered, we measure their power by calibration. Each of the three seed games is first run through the whole battery unmodified, and every applicable test passes. We then inject eight classes of known defect, twelve instances in total, into the hooks of every seed game to which they apply, which yields 30 mutants, and run every test again. Since all variants of a family execute the same hook code, a defect in a hook is shared by every encoding, rule, and size variant of the family. We therefore inject each defect into every variant of the family rather than into a single variant, as injecting into one variant only would make the Encoding test appear to catch every defect and would measure the injection rather than the test. The one exception is the last row of Table 6, which is scoped to a single encoding variant because this is precisely the situation that the Encoding test tests for. The Duplicate test is a predicate over pairs of games rather than over a single game, and is therefore reported separately below.

The battery rejects all 30 injected mutants. Three results in Table 6 deserve attention.

First, an inverted verdict is caught only by the agreement check. When the hook that decides the winner is inverted throughout a family, rewards still sum to zero, illegal actions are still penalised, every rendered label is still accepted, every episode still terminates, the encoding variants still agree with one another, and an outcome-reversing rule variant is still an exact flip of its parent. Consequently, every mechanical replay test passes, and only the comparison against an independently written implementation of the same specification detects the defect. This is the strongest evidence

Table 5: Candidates eliminated by each test across all synthesis runs. Ran on is the number of families with a stored record for the test, and Rejected the number it turned away.

Test	Ran on	Rejected	What was rejected
Not triggered in this batch			
Encoding	69	0	NA
Rule	68	0	NA
Outcome	69	0	NA
Information hiding	43	0	NA
Triggered			
Playability	33	1	a negotiation family: 0.23 trades per episode (threshold 0.5), decisive in 0.20 of episodes (threshold 0.25)
Agreement	42	1	a deduction family: 30 actions against 31 in the re-implementation, reviewed as an ambiguity in the specification
Duplicate (pairs)	35	3	three families whose outcomes matched an admitted family on all 60 shared seeds
Checks outside the seven tests			
Static safety	80	4	proposals using a banned identifier, never reached the replay tests
Degeneracy flag	61	1	a family with a first-mover win share of 0.054, outside the admissible band

Table 6: Injected defects on the three seed games and the tests that rejected them. Each cell counts the mutants of the row that the test rejected, so one mutant may appear in several columns. Columns follow Table 4.

Injected defect	n	Enc	Rule	Out	Hide	Play	Agr	Caught
Outcome and reward hooks								
Verdict inverted	3	0	0	0	0	0	3	3/3
Rewards not zero-sum	6	0	3	6	0	1	6	6/6
Never terminates	3	0	1	3	0	1	3	3/3
Action rendering								
Action labels corrupted	6	0	3	6	0	1	6	6/6
Hidden state								
Opponent's private state leaked	4	0	0	0	4	0	0	4/4
Variant-level defects								
Rule variant has no effect	3	0	3	0	0	0	0	3/3
Menu not at parity, bot never trades	2	0	1	0	0	2	2	2/2
One encoding settles differently	3	3	0	0	0	0	0	3/3
Total	30	3	11	15	4	5	20	30/30

that the agreement check is effective, and it justifies the cost of the check even though it turned away only one candidate.

Second, three tests are the sole detector of a defect class: Rule for a rule variant with no effect, Encoding for an encoding that settles differently, and Information hiding for a leak, which no other test notices because a leak changes what a player sees without changing any trajectory. The two menu defects reproduce the failure mode that motivated the Playability test: pricing the trade menu by quantity rather than by base value means that any swap that helps the proposer must cost the responder under their own scoring, so a score-maximising bot never trades. Both mutants fail Playability with 0.00 trades per episode and are also caught by the Agreement test, so Playability provides a direct check of this failure mode rather than the only one.

Third, the Duplicate test behaves as specified when exercised directly. A planted clone of an admitted game matches on 60 of 60 shared seeds and is flagged, two genuinely different games on the same board are not, and the one pair flagged in the ledger reproduces at 60 of 60 on the admitted

configuration but differs on 11 of 60 once the deck is enlarged, which shows that the collision is a property of the configuration rather than of the two specifications.

Dependence on the seed set and the driver. To check this dependence, we repeated the whole injection matrix with the seed set shifted and the driver's random stream shifted independently, which changes both the seeds of Table 4 and the action sequences drawn on them. Every cell of Table 6 is unchanged, and the three seed games still pass every applicable test unmodified. None of the conclusions in this subsection therefore depends on the particular seeds of Table 4.

Manual review. The agreement check compares two readings of a specification and cannot detect a misreading that both share. To bound this, we read the specification and the hook implementation of ten admitted games side by side, four grid games (Chop-3 Scorers, Clampdown, Pivot Flips, Trap-Go Threshold), four betting games (Modular Sum Showdown, Bitwise XOR High, Target Sum, Median Dominance), and two negotiation games (K-of-Each Set Collection, Tiered Diminishing Returns), and tested every clause whose reading was in doubt on constructed positions. Eight implement their specification exactly. Trap-Go Threshold adds a termination clause that the specification leaves open, ending the game when the player to move has no legal move, and its rules text states this clause. Tiered Diminishing Returns rounds the inventory score to the nearest integer, which the specification does not, and the rounding changes the winner in 12 of 20,000 random start-and-end pairs. Its rules text gives the unrounded formula, and the score shown to the players at every turn is the rounded value that the engine settles on.

In both cases the value the player is shown at every turn is the value the engine settles on, so the reward stays consistent with what the policy observes, and what the deviation moves is the specification-to-implementation translation rather than the game the model learns. Both deviations are also of a kind that a stronger re-implementation model would be more likely to expose, since neither is ambiguous in the specification text; the check's power is limited by the re-implementer rather than by the protocol, and it improves as the model does.

A.4 Corpus composition

A.4.1 Admitted games

Across all synthesis runs, the designer proposed 80 games. Of these, 76 were implemented within the attempt budget and 75 passed the replay tests, with an average of 1.7 engineer attempts per game. Every one of the 26 admitted games agrees with its independent re-implementation on every replayed outcome. Table 7 lists the 26 admitted games by template, with a one-line description of the rule that distinguishes each game from its template's seed game. Full rule texts are included in the corpus release. The complexity reported in §5.2 is game-tree complexity, $\log_{10} \mathrm{GTC} \approx \bar{d} \log_{10} \bar{b}$, where $\bar{b}$ is the mean branching factor and $\bar{d}$ is the mean game length under random play (Allis, 1994).

A.4.2 Training, validation, and held-out variants

The effect size of a rule or size variant is defined as the fraction of 60 seed-paired episodes whose outcome differs from that of the parent game under the same action sequence. All 29 families are used for distillation, and 22 of the synthesised families are sampled by the game sampler during the self-play RL stage. Within a family, the distillation data consist of the base game with a random encoding per episode, up to two rule variants with effect size in $[0.2, 0.95]$, and the first size variant. Two fixed encodings form a validation split, while the transposed encoding, the rule variant with the highest effect size, and the last size variant are held out as a test split and are not trained on.

B Proofs and additional theoretical analysis

B.1 Proof of Lemma 1

We write $S_i = \nabla_\theta \log \pi_\theta(\tau_i)$ and $\hat{g}_i = (R(\tau_i) - b_i)\, S_i$. Since the baseline b_i is a function of the other returns of the batch and of a prior fitted on earlier batches, it is independent of τ_i given the

Table 7: Admitted games by template.

Key	Name	Rule in one line
Grid placement (seed: Tic-Tac-Toe)		
ANTICL	Anti-Clump Diagonals	A stone may not touch one's own stones orthogonally. The first diagonal line of K wins, and a player with no legal move loses.
CHOP	Chop-3 Scorers	A row or column that reaches a threshold of one's own stones is cleared. The first to complete the target pattern wins.
CLAMP	Clampdown	An opponent stone between two of one's own is captured. The first to the target number of captures wins.
CROSSL	Crosslink	One side connects north to south and the other west to east. The first connection wins.
FIVMIS	Cross-Exception Misère	Both players place the same mark. Completing a straight line of K loses.
MAJSEG	Majority Segments	The board is cut into segments of K cells. The player holding the majority in more segments wins.
NEUTRW	Neutral Win, Hot Loss	Each turn places a neutral or a hot stone. A line of neutral stones wins and a line of hot stones loses.
NOSQRE	No-Squares Misère	Completing a one-colour $k \times k$ square loses.
PIVOT	Pivot Flips	A placed stone flips the stones on its orthogonal lines. The first line of K wins.
QUARN	Quarantine	The board is split into quadrants and the winning condition must be met inside the designated one.
SWEEPR	Row-Column Sweeper	A placement clears the rest of its row and column. The first to complete the target pattern wins.
TRAPGO	Trap-Go Threshold	Connected opponent groups whose liberties fall below a threshold are captured.
TWINRS	Twin Rows	Lines count only as twin pairs. The first to collect R pairs wins.
Betting with a showdown (seed: Kuhn Poker)		
BITXOR	Bitwise XOR High	The showdown is won by the higher bitwise XOR of the hand's ranks.
CENTER	Center-Seek High	The showdown is won by the card closest to a target value.
CLUST	Clustered High	The showdown is won by the hand whose ranks are closest together.
DUPES	Duplicate Power Bonus	Repeated ranks score as a power of their count, and the higher total wins the showdown.
MAXGAP	Far Apart Wins	The showdown is won by the larger gap between the highest and lowest card.
MEDIAN	Median Dominance	The showdown is won by the higher median rank.
MODSUM	Modular Sum Showdown	The showdown is won by the higher sum of ranks modulo M.
PARITY	Parity Majority High	The showdown is won by the hand with more cards of the preferred parity, then by the higher card.
TARGET	Target Sum, Don't Bust	The showdown is won by the rank sum closest to a target without exceeding it.
Resource negotiation (seed: Simple Negotiation)		
CAPWST	Caps and Waste	Units of a resource above a cap are wasted. The larger growth in inventory value wins.
PAIRED	Paired Complements	Resources held in pairs earn a bonus. The larger growth in inventory value wins.
SETK	K-of-Each Set Collection	Each complete set of K of every resource earns a bonus. The larger growth in inventory value wins.
TIERD	Tiered Diminishing Returns	A resource's value diminishes by tier. The larger growth in inventory value wins.

policy, and $\mathbb{E}[\hat{g}_i] = \mathbb{E}[R(\tau_i)S_i] - \mathbb{E}[b_i]\,\mathbb{E}[S_i] = \nabla_\theta J$ because $\mathbb{E}[S_i] = 0$. For the variance,

$$\mathrm{Var}[\hat{g}_i] \;=\; \mathbb{E}\big[(R(\tau_i) - b_i)^2\,\|S_i\|^2\big] - \|\nabla_\theta J\|^2 \;=\; \mathbb{E}\big[(R(\tau_i) - b_i)^2\big]\,\mathbb{E}\big[\|S_i\|^2\big] - \|\nabla_\theta J\|^2,$$

where the second equality follows from the stated assumption. Expanding about μ_g,

$$\mathbb{E}\big[(R(\tau_i) - b_i)^2\big] \;=\; \mathbb{E}\big[(R(\tau_i) - \mu_g)^2\big] + \mathbb{E}\big[(b_i - \mu_g)^2\big] - 2\,\mathbb{E}\big[(R(\tau_i) - \mu_g)(b_i - \mu_g)\big],$$

where the cross term vanishes because b_i is independent of $R(\tau_i)$ and $\mathbb{E}[R(\tau_i) - \mu_g] = 0$. Hence, $\mathrm{Var}[\hat{g}_i] = \big(\sigma^2 + \mathbb{E}[(b_i - \mu_g)^2]\big)\,\mathbb{E}[\|S_i\|^2] - \|\nabla_\theta J\|^2$, which is an increasing affine function of the mean squared error of b_i.

For the second claim, we write $w = K'_g/(K'_g + \kappa)$ so that $b_i - \mu_g = w\,(\bar{y}_{g,-i} - \mu_g) + (1 - w)\,(m_g - \mu_g)$. The first term is the sampling error of the leave-one-out mean, with variance σ^2/K'_g, and the second term is the error of the prior, with mean square τ^2 by definition. The two terms are uncorrelated, since the prior is fixed before the batch is sampled, so

$$\mathbb{E}\big[(b_i - \mu_g)^2\big] \;=\; w^2\,\frac{\sigma^2}{K'_g} + (1 - w)^2\,\tau^2.$$

This is a convex quadratic in w, which is minimised at $w^\star = \tau^2/(\tau^2 + \sigma^2/K'_g) = K'_g/(K'_g + \sigma^2/\tau^2)$, that is, at $\kappa^\star = \sigma^2/\tau^2$, where its value is $\sigma^2\tau^2/(K'_g\tau^2 + \sigma^2) = \sigma^2/(K'_g + \kappa^\star)$. The two limiting cases are $w = 1$, the leave-one-out mean with error σ^2/K'_g, and $w = 0$, the prior with error $\tau^2 = \sigma^2/\kappa^\star$, and both exceed $\sigma^2/(K'_g + \kappa^\star)$.

B.2 Error analysis of the shrinkage baseline

The proof above gives the mean squared error of the baseline in closed form,

$$\mathrm{MSE}(w) \;=\; \mathbb{E}\big[(b_i-\mu_g)^2\big] \;=\; w^2\,\frac{\sigma^2}{K'_g} + (1-w)^2\,\tau^2, \qquad w=\frac{K'_g}{K'_g+\kappa}, \tag{7}$$

and three consequences of this expression are used in the paper.

First, the decomposition does not assume that the prior is correct. Since τ^2 is defined as the mean squared error of the prior that is actually used, it includes both the bias of the linear model, which cannot represent interactions between fields, and its lag, since the prior is fitted on earlier batches. The normal model of §4.2 is used only to motivate the choice $\kappa^\star = \sigma^2/\tau^2$. For any fixed κ, the baseline is independent of the action, the gradient remains unbiased, and equation 7 gives its error.

Second, the error is flat near its minimum. Since equation 7 is a quadratic in w with second derivative $2(\sigma^2/K'_g+\tau^2)$,

$$\mathrm{MSE}(w)-\mathrm{MSE}(w^\star) \;=\; (w-w^\star)^2\,\Big(\frac{\sigma^2}{K'_g}+\tau^2\Big). \tag{8}$$

This observation has two uses. On the one hand, a fixed κ that is within a factor of two of $\kappa^\star$ costs little, which is why the main runs fix $\kappa=4$. On the other hand, replacing $\kappa^\star$ by a plug-in estimate $\hat\kappa$ moves w by some δ and costs $\delta^2(\sigma^2/K'_g+\tau^2)$, so the estimated variant of the estimator is not expected to differ from the fixed one unless $\hat\kappa$ is far off.

The quantities in equation 7 are estimated during training. The within-group variance σ^2 is estimated by pooling the sample variances of the groups of a batch, and $\tau^2=\mathbb{E}[(\mu_g-m_g)^2]$ is estimated by the method of moments,

$$\hat\tau^2 \;=\; \mathrm{mean}_g\Big[\big(\bar y_g-m_g\big)^2-\hat\sigma^2/K_g\Big], \tag{9}$$

where $\bar y_g$ is the full group mean and the second term removes its sampling noise. Both estimates are smoothed across batches, and $\hat\kappa=\hat\sigma^2/\hat\tau^2$. The variant of CRAB that uses $\hat\kappa$ does so with one batch of lag, so that the baseline of a batch never depends on its own returns. Because τ^2 is measured against the prior that is actually used, it includes the prior's bias and lag. The encoding variance $\hat\tau^2_{\mathrm{enc}}$ is computed on the same returns split by encoding, as the variance across encodings of the mean return within each group, corrected for sampling noise in the same way.

Third, since these quantities are measured, the error can be evaluated empirically. Table 8 reports $\hat\sigma^2$, $\hat\tau^2$ of equation 9, $\hat\kappa=\hat\sigma^2/\hat\tau^2$, and $\hat\tau^2_{\mathrm{enc}}$ on Qwen3-4B-Base with $G=5$, averaged over steps 31 to 60 of the main configuration with $\kappa=4$ and of the variant that uses $\hat\kappa$ with one batch of lag. With $K'_g=4$, the leave-one-out mean alone has error $\sigma^2/K'_g\approx 0.23$, the prior alone has error $\tau^2\approx 0.16$, and the shrinkage estimator has error 0.10 at either $\kappa=4$ or $\kappa=\hat\kappa$. The estimate $\hat\kappa$ lies between 5 and 8 from step 10 onwards, so $\kappa=4$ is within a factor of two of the estimated optimum, and by equation 8 the difference in error between the two runs is below 0.003. Their scores are consistent with this: at steps 20, 40, and 60 they differ by -1.6, -1.7, and $+0.1$ points, with no consistent sign. The encoding variance $\hat\tau^2_{\mathrm{enc}}$ decreases from 0.70 at step 15 to 0.50 at step 30 and stays there, indicating that the policy moves towards encoding invariance early in training but remains some distance from it at this budget. Note that these are moment estimates from the returns of each batch rather than held-out prediction errors, and that the two runs are single seeds.

Table 8: Estimated variances of the shrinkage baseline on Qwen3-4B-Base, steps 31 to 60, and the baseline error implied by equation 7.

Run	$\hat\sigma^2$	$\hat\tau^2$	$\hat\kappa$	$\hat\tau^2_{\mathrm{enc}}$	MSE at κ used
$\kappa=4$	0.91	0.16	6.4	0.50	0.098
$\kappa=\hat\kappa$	0.94	0.19	5.4	0.49	0.099

Fourth, the error can be measured directly rather than inferred from equation 7. The claim under test is that of Lemma 1: the shrinkage baseline is an interior point between the leave-one-out mean at $w=1$ and the prior at $w=0$, its error is smaller than that of either endpoint, and equation 7 gives its size. To measure this, we freeze the step-40 and step-120 checkpoints of the run with $\kappa=4$ and draw

independent rollout batches from each with the training sampler and the training hyperparameters ($G = 5$, $K'_g = 4$, temperature 1, response budget 16,384 tokens), with no parameter update: 35 and 96 batches of the size that the trainer hands to one lane, i.e., 535 and 1,500 games for the two steps, respectively. Since μ_g is fixed, every baseline can be recomputed offline on the same returns, so the differences between rows come from the baseline alone. Because b_i never uses R_i, $\mathbb{E}[(R_i - b_i)^2] = \sigma^2 + \mathbb{E}[(b_i - \mu_g)^2]$, and subtracting the pooled within-group variance ($\hat{\sigma}^2 = 0.95$ and 0.92 over the whole probe) gives the error of each baseline without a proxy for μ_g. Two baselines are compared as a paired difference of $(R_i - b_i)^2$ on the same trajectories, which removes the variation they share and does not depend on $\hat{\sigma}^2$. Intervals are 95% bootstrap intervals over (batch, group) blocks. The factored prior is fitted online, lane by lane, on the earlier batches of the probe, as in training, with the first 20 batches excluded as warm-up. The closed form equation 7 is evaluated at the $\hat{\sigma}^2$ above and at $\hat{\tau}^2 = 0.15$ and 0.12 from equation 9 on the same rollouts, which give $\hat{\kappa} = 6.3$ and 7.4. Table 9 reports the measured errors and Table 10 sweeps κ on the same rollouts. Three findings support the claim.

The interior point beats both endpoints. At step 120 the leave-one-out mean has a measured error of 0.240, the prior 0.129, and CRAB with $\kappa = 4$ 0.096. The paired differences agree, with intervals that exclude zero: CRAB is 0.143 $[0.129, 0.157]$ below the leave-one-out mean and 0.033 $[0.006, 0.063]$ below the prior. Step 40 gives the same ordering, 0.233, 0.148, and 0.093, again with paired intervals that exclude zero.

The closed form predicts the measured error. Evaluated at the $\hat{\sigma}^2$ and $\hat{\tau}^2$ of the same rollouts, equation 7 is within 0.010 of the measurement on every row of Table 9, and the measured error of the estimator used in the main runs, 0.093 and 0.096, agrees with the 0.098 that Table 8 infers from equation 7 during training. The probe also reproduces the moment estimates of the training run, $\hat{\sigma}^2 = 0.95$ and 0.92 against 0.91, and $\hat{\kappa} = 6.3$ and 7.4 against 6.4, which serves as a check on the probe itself.

The fixed κ costs little. Table 10 sweeps κ on the same rollouts. The measured curve is a shallow basin with its minimum at $\kappa = 8$, next to the $\hat{\kappa}$ of these rollouts, and it is flat across the range that equation 8 predicts to be flat: moving from $\kappa = 4$ to the minimum changes the error by 0.003 at step 40 and by 0.009 at step 120, compared with a gap of about 0.14 to the leave-one-out mean.

The lemma bears on the error of the baseline, which is what these tables measure, and the comparison between estimators in training is the empirical one of Table 2.

Table 9: Measured error of the baseline under a frozen policy, at the step-40 and step-120 checkpoints of the CRAB run of Table 8. Measured MSE is $\mathbb{E}[(R_i - b_i)^2] - \hat{\sigma}^2$, the equation 7 column is the closed form at the $\hat{\sigma}^2$ and $\hat{\tau}^2$ of the same rollouts, and Δ is the paired difference against CRAB with $\kappa = 4$, positive when the row has the larger error, with 95% bootstrap intervals in brackets.

Step	Baseline	w	Measured MSE	equation 7	Δ vs CRAB, $\kappa = 4$
40	CRAB, $\kappa = 4$	0.50	0.093 [0.044, 0.142]	0.097	–
	CRAB, $\kappa = \hat{\kappa}$	0.39	0.089 [0.043, 0.133]	0.092	−0.005 [−0.013, 0.004]
	Leave-one-out mean	1	0.233 [0.166, 0.300]	0.238	0.139 [0.115, 0.163]
	Factored prior	0	0.148 [0.101, 0.197]	0.151	0.055 [0.006, 0.106]
120	CRAB, $\kappa = 4$	0.50	0.096 [0.065, 0.127]	0.088	–
	CRAB, $\kappa = \hat{\kappa}$	0.35	0.087 [0.058, 0.115]	0.080	−0.009 [−0.015, −0.001]
	Leave-one-out mean	1	0.240 [0.195, 0.281]	0.230	0.143 [0.129, 0.157]
	Factored prior	0	0.129 [0.096, 0.160]	0.124	0.033 [0.006, 0.063]

B.3 ENCODING SYMMETRY

Fix a game and let $\mathcal{G}$ be its set of encodings. Each $e \in \mathcal{G}$ is a bijection on rendered observations and on action labels, and the kernel of the template applies it after the game logic has run (§4.1): the state is stored in a canonical form, the hooks act on that form, and e renders the state and reads the action. Since the composition and inversion of such maps are again such maps, $\mathcal{G}$ is a group, and for every state s and action a the canonical successor and outcome of (s, a) are those of $(e(s), e(a))$. Three statements follow from this.

Table 10: The rollouts of Table 9 with κ swept. The first and last rows are the two endpoints of Lemma 1, and the equation 7 columns evaluate the closed form at the $\hat{\sigma}^2$ and $\hat{\tau}^2$ of the same rollouts ($\hat{\kappa} = 6.3$ and 7.4).

κ	w	Step 40, measured	equation 7	Step 120, measured	equation 7
0 (leave-one-out)	1	0.233 [0.166, 0.300]	0.238	0.240 [0.195, 0.281]	0.230
0.5	0.89	0.185 [0.121, 0.248]	0.190	0.192 [0.150, 0.232]	0.183
1	0.80	0.154 [0.093, 0.214]	0.158	0.161 [0.121, 0.199]	0.152
2	0.67	0.118 [0.063, 0.173]	0.122	0.124 [0.088, 0.159]	0.116
4	0.50	0.093 [0.044, 0.142]	0.097	0.096 [0.065, 0.127]	0.088
8	0.33	0.090 [0.047, 0.131]	0.094	0.087 [0.059, 0.115]	0.081
16	0.20	0.103 [0.061, 0.143]	0.106	0.095 [0.066, 0.121]	0.088
∞ (prior)	0	0.148 [0.101, 0.197]	0.151	0.129 [0.096, 0.160]	0.124

First, values are invariant. Since V is computed from the canonical state by the hooks (§4.2), we have $V(e(s)) = V(s)$. Similarly, the minimax value of the game from a seat is a function of the canonical game tree, which e does not change.

Second, the group maps optimal policies to optimal policies. For a policy π and $e \in \mathcal{G}$, define $\pi^e(e(a) \mid e(s)) = \pi(a \mid s)$. By the commutation above, the distribution over canonical trajectories induced by π^e playing under encoding e equals the distribution induced by π playing under the identity, for either seat and against any opponent transported in the same way. Since expected returns are functions of canonical trajectories, they agree, and a policy that is optimal under the identity is therefore transported to a policy that is optimal under e.

Third, equivariant policies have encoding-independent returns. If $\pi^e = \pi$ for every e, then playing π under e is the same as playing π^e under e, which by the previous statement has the expected return of π under the identity. Hence, the expected return of a group g does not depend on the encoding, the variance across encodings of the mean return within a group is zero, and τ^2_{enc} of §4.2 vanishes. Conversely, a nonzero τ^2_{enc} indicates that the policy treats some renderings of the same game differently.

B.4 Equivariance and the encoding variants

The encoding group of Appendix B.3 also characterises what training under a fresh encoding per episode aims at, and why it does not enlarge what has to be learned. Fix a game with encoding group $\mathcal{G}$, and for a policy π write π^e for its transport by $e \in \mathcal{G}$ as above. The *orbit average* of π is the mixture

$$Q\pi \;=\; \frac{1}{|\mathcal{G}|} \sum_{e \in \mathcal{G}} \pi^e,$$

which is itself a policy, and since $e' \in \mathcal{G}$ permutes the terms of the sum, $(Q\pi)^{e'} = Q\pi$. Therefore, Q maps every policy to an equivariant one and fixes the equivariant ones, that is, Q is a projection onto the equivariant policies. Let $L_e(\pi)$ be the distillation loss of §4.2 on teacher trajectories rendered under encoding e, i.e., the cross-entropy of π against the action of π_{T}. Drawing the encoding uniformly per episode, as the distillation data do, minimises the orbit average of the loss, $\bar{L}(\pi) = |\mathcal{G}|^{-1} \sum_e L_e(\pi)$. The argument assumes that the teacher is equivariant, so that its trajectories and actions are canonical objects rendered under e. Three facts follow.

First, $\bar{L}$ is invariant under transport. By the commutation of Appendix B.3, $\pi^{e'}$ evaluated on trajectories rendered under e equals π evaluated on the same trajectories rendered under $e'^{-1} \circ e$, so $L_e(\pi^{e'}) = L_{e'^{-1} \circ e}(\pi)$, and averaging over e gives $\bar{L}(\pi^{e'}) = \bar{L}(\pi)$.

Second, the orbit average does not increase the loss. Since the cross-entropy is convex in the policy's conditional distributions, Jensen's inequality together with the first fact gives $\bar{L}(Q\pi) \leq |\mathcal{G}|^{-1} \sum_e \bar{L}(\pi^e) = \bar{L}(\pi)$. A minimiser of $\bar{L}$ can therefore be taken to be equivariant, and training under random encodings targets an equivariant policy, which by Appendix B.3 is also where the optimal self-play policy lies.

Table 11: Non-game control data: verified-correct teacher traces on non-game reasoning, by capability and source (training splits only), decontaminated against every evaluation benchmark and subsampled to the GAMESMITH (matched) token budget.

Capability	Source (train split)	Traces
Deductive logic	ReClor	7,666
	LogiQA	6,163
	ProofWriter	2,334
Spatial & state-tracking	SpartQA	6,339
	StepGame	184
Competition mathematics	MetaMathQA	7,889
	OpenMathInstruct-2	5,777
	NuminaMath-CoT	3,690
Total		**40,042**

Third, the equivariant class is no larger than the full class. Let Π be the set of policies that the model can represent, and measure distance by $d(\pi, \pi') = \max_s \sum_a |\pi(a \mid s) - \pi'(a \mid s)|$. Since transport by e is a relabelling of states and actions, we have $d(\pi^e, \pi'^e) = d(\pi, \pi')$, and the triangle inequality gives $d(Q\pi, Q\pi') \leq d(\pi, \pi')$. The image under Q of an r-cover of Π is an r-cover of $Q\Pi$, so the covering number of $Q\Pi$ is at most that of Π, and the covering-number bounds on the generalisation gap (Zhou, 2002; Bartlett & Mendelson, 2003) for the equivariant class are no larger than those for Π. This is the same argument that Qin et al. (2022) make for permutation symmetry in auctions and van der Knaap et al. (2026) for reflection symmetry in control, applied here to the encoding group, which is finite and known exactly for every game because the kernel implements it.

Two limitations of this argument are worth stating. First, the policy is not constrained to $Q\Pi$: an LLM reads rendered text and is not equivariant by construction, so random encodings change the target of training rather than the class, and $\hat{\tau}^2_{\text{enc}}$ of Appendix B.2 measures how far the trained policy still is from that target. This is also why encodings are needed as training variants at all. For an equivariant model, one rendering of a game would be as good as all of them, but a model that has to learn the invariance learns it from the renderings it sees, and these are the cheapest variants in the corpus, since they add no game to admit and no reward to verify. The second limitation is quantitative. A reduction in sample complexity by a factor related to $|\mathcal{G}|$ is known for linear and kernel models (Elesedy & Zaidi, 2021) and under the general framework of Chen et al. (2020), but it is not claimed here for a transformer policy. What the argument does establish is that the target reached by training on random encodings is the same game-theoretic policy in every rendering, that this target is no harder to represent than the policy for one rendering, and that once the policy is equivariant, a trajectory under any encoding carries the same information about every other. This is the sense in which the corpus counts encoding variants separately from rule and size variants.

C ADDITIONAL IMPLEMENTATION DETAILS

C.1 NON-GAME CONTROL DATA

The *non-game* control (Table 1) isolates whether the transfer is due to distillation of a strong teacher's reasoning rather than to something specific to games. It uses the *same* teacher, decoding, and $\langle$think$\rangle$ + `\boxed` output format as the GAMESMITH SFT data, but on non-game reasoning prompts spanning the capability types that the games exercise. Prompts are drawn only from the *training* splits of the sources in Table 11 and sampled with the teacher, and only teacher solutions that are verified correct against the gold answer are kept. The retained set is subsampled to the GAMESMITH (matched) token budget.

Before training, we remove any prompt that overlaps with the evaluation data, checked against *every* benchmark in Table 1 (the five mathematics sets, MMLU-Pro, GPQA-Diamond, and the six BBH tasks). A prompt is dropped if it triggers any of three independent checks: (i) exact match after normalisation, (ii) a shared 13-gram with an evaluation question, or (iii) an embedding near-duplicate, with cosine similarity ≥ 0.85 to the nearest evaluation question under a sentence encoder.

Of 26,904 candidate prompts, 111 were dropped (14 exact, 67 by 13-gram, 30 by embedding). These were concentrated in the mathematics sources, whose items are frequently rephrasings of MATH/AMC/GSM8K, whereas the logical and spatial sources triggered essentially no overlap. We err on the side of dropping.

C.2 Hyperparameters, software, and hardware

Table 12 lists the settings of the three stages. Every distillation run is trained with the same optimiser settings for a fixed number of optimiser steps (2,056 for the settings of Table 1, 2,048 for the SPIRAL setting) and is evaluated at its final weights. No checkpoint selection is applied to any distillation run, including those of Figure 3, and intermediate checkpoints are kept only for crash recovery.

Table 12: Hyperparameters, software, and hardware of the three stages.

Stage	Setting	Value
Distillation (SFT)	optimiser, learning rate	AdamW, 10^{-5}, cosine to zero, warmup 3%
	effective batch	32 sequences, per-device batch 1 with gradient accumulation
	context	16,384 tokens, no truncation of any record
	precision, memory	bf16, gradient checkpointing, fused cross-entropy
	parallelism	data parallel for 4B, ZeRO-2 for 8B and 12B
	GPUs	4 GPUs for 4B and 8B, 8 GPUs for 12B
Self-play (RL)	estimator	CRAB with $\kappa = 4$, $\lambda = 0.5$, and $G = 5$ episodes per sampled variant, each with a fresh seed and encoding. The RAE control on the GAMESMITH corpus keeps $G = 5$ and every other setting and replaces only the estimator.
	optimiser	learning rate 10^{-6}, PPO clip ratio 0.2, no KL or entropy term
	sampling	temperature 1.0, top-p 1.0, at most 50 turns per episode
	context	prompt up to 4,096 tokens and response up to 16,384 in a 20,480-token window.
	over-length	a response beyond 15,360 tokens receives -1.5, folded into its return before the baseline is subtracted.
	batch	128 transitions (decisions) per optimiser step, 200 steps
	software	verl 0.6.1 with vLLM 0.10.2 rollouts, FSDP actor
	GPUs	4 GPUs for the 4B model, 8 GPUs with tensor parallelism 2 for the 8B, 9B, and 12B models
Evaluation	decoding	4 samples, temperature 0.6, top-p 0.95, 8,192 tokens
	software	vLLM 0.10.2, one GPU per checkpoint
	wall-clock	about 5 hours for the 13 benchmarks on an 8B checkpoint

C.3 Compute budget

All training and evaluation runs use GPUs with 16,896 CUDA cores, 132 streaming multiprocessors, and 80 GB of memory. Each run uses a single node with 8 GPUs, with one GPU for evaluation and 4 or 8 GPUs for training, as specified in Table 12. Compute is reported in GPU hours, calculated as wall-clock hours multiplied by the number of GPUs. Training estimates are derived from per-step timings in the logs. All estimates are rounded to two significant figures.

The main training and evaluation experiments require approximately 9,800 GPU hours. The twelve self-play runs in Table 2 account for approximately 9,100 GPU hours at the 200-step budget. The sixteen distillation runs in Table 1 require approximately 360 GPU hours in total, and evaluation of the checkpoint grids of Table 2 requires a further 380 GPU hours. The eight $G = 1$ runs of Appendix D.4 add approximately 4,200 GPU hours, and the game-side evaluation of Appendix D.7 about 200 GPU hours on single GPUs. In total, the study uses approximately 14,000 GPU hours across all experiments reported in the main paper and appendices.

C.4 Evaluation protocol

Table 13 lists the 13 benchmarks, their sizes, and their groups. Every benchmark is evaluated on its full test set, except for MMLU-Pro, for which a fixed random subset of 1,000 questions is used. Each question is sampled 4 times at temperature 0.6 and top-p 0.95 with an 8,192-token generation budget under vLLM. A sample is considered correct if its final `\boxed` answer matches the reference, under a symbolic-equivalence grader for mathematics and exact match after normalisation otherwise. pass@1 is the mean correctness over the 4 samples, and the headline number is the unweighted mean of the 13 per-benchmark pass@1 values. The same protocol is applied to every checkpoint in the paper, including the base models, with a context window of 32,768 tokens for distillation checkpoints and 12,288 for self-play checkpoints, both of which are larger than any prompt plus the generation budget.

Table 13: Evaluation benchmarks, sizes, and groups. The five mathematics sets are the ones distributed with the SPIRAL evaluation code.

Group	Benchmark	Questions
Mathematics	AIME 2024	30
	AMC 12 (2022–2023)	83
	MATH-500	500
	Minerva Math	272
	OlympiadBench	675
Knowledge	MMLU-Pro (fixed random subset)	1,000
	GPQA-Diamond	198
Logical reasoning	BBH Logical Deduction (3 obj.)	250
	BBH Logical Deduction (5 obj.)	250
	BBH Web of Lies	250
Spatial & tracking	BBH Tracking Shuffled Objects (3 obj.)	250
	BBH Geometric Shapes	250
	BBH Navigate	250

C.5 Assets and licences

Table 14 lists the models, software, and datasets used in this work, together with their licences. ReClor and LogiQA are licensed for non-commercial research use and are used only to build the non-game control, which is not redistributed. The synthesised corpus contains only game specifications and code produced by the pipeline of §4.1.

D Additional empirical results

This appendix supplements §5 with the diversity and complexity of the corpus, diagnostics of the Format control, and the self-play stage on the games themselves: the evaluation curves of the three pipelines over the budget, the rate of draws and the advantage signal, the comparison of the two estimators with one episode per variant, and the win rates of the trained policy on variants that it never trained on.

D.1 Corpus diversity and complexity

Figure 4 summarises the diversity and complexity of the corpus. Embedding every family by its rule text shows that the synthesised games spread across all 3 genres, while the 3 SPIRAL games occupy only a small region. In terms of effective count, the Vendi score by mechanic is 9.1 for the corpus against 2.5 for the three SPIRAL games, and 5.1 against 2.2 on a behavioural descriptor (decisiveness, first-mover edge, game length, and branching). Rule variation changes outcomes: the fraction of episodes whose outcome is flipped by a rule change ranges from 0.02 to 1.00 (median 0.63), whereas encoding variants preserve outcomes exactly. Game-tree complexity (Appendix A.4.1) spans $[0.7, 68]$ across the 336 variants: size variants supply the top of the range, raising the com-

Table 14: Assets and licences.

Asset	Licence
Models	
Qwen3-4B-Base, Qwen3-8B-Base	Apache 2.0
Qwen3-32B (teacher, independent re-implementation)	Apache 2.0
Mistral-Nemo-Instruct-2407	Apache 2.0
GLM-4-9B-0414	MIT
GPT-5 through its API (designer and engineer)	OpenAI terms of use
Software and code	
TextArena (seed games)	MIT
SPIRAL (evaluation code, mathematics sets, RAE)	MIT
verl, vLLM (training, inference)	Apache 2.0
Evaluation datasets	
MATH-500, MMLU-Pro, BBH	MIT
AIME 2024, AMC 12 (2022–2023), Minerva Math	as distributed with SPIRAL
OlympiadBench	MIT
GPQA-Diamond	CC BY 4.0
Non-game control datasets	
ReClor	non-commercial research use
LogiQA	CC BY-NC-SA 4.0
ProofWriter, OpenMathInstruct-2	CC BY 4.0
SpartQA, StepGame, MetaMathQA	MIT
NuminaMath-CoT	Apache 2.0

plexity in every grid family and the ceiling from 52 to 68, betting families keep the game tree small, and negotiation families fill the middle.

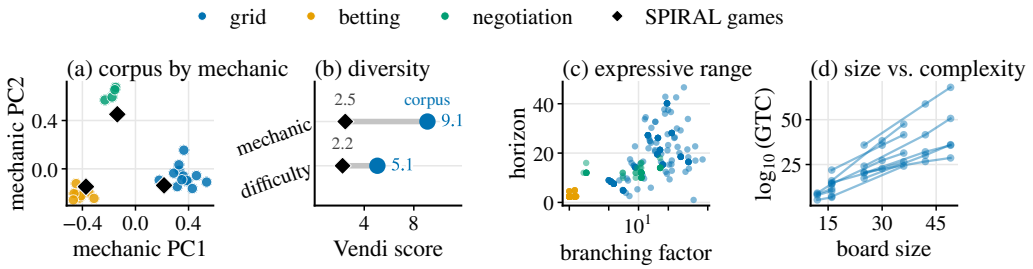

Figure 4: Corpus diversity and complexity. **(a)** Families embedded by rule text (PCA), coloured by genre, with the 3 SPIRAL games shown as black diamonds. **(b)** Vendi score of the corpus and of the SPIRAL games under a mechanic and a difficulty lens. **(c)** Branching factor and horizon of all variants and base games. **(d)** Game-tree complexity against board size, with one line per grid family.

D.2 Per-benchmark results

Tables 15, 16, 17, and 18 present, for each model of Table 1, the per-benchmark results that it summarises by capability group.

D.3 Diagnostics of the Format control

The Format control of Table 1 scores below the base model on every model, by 16.7 points on Qwen3-4B-Base and by 34.6 to 40.2 points on the other three. This control is derived mechanically from the GameSmith distillation data by deleting the reasoning block of every response and keeping only the final `\boxed` action, so that the two settings share the same 8,208 records, the same eight epochs, and the same optimiser settings. Table 19 reports generation-level diagnostics for this control under the evaluation protocol of §5.1 ($k = 4$, 8,192 maximum new tokens, temperature

Table 15: Per-benchmark results for Qwen3-4B-Base (pass@1 %, 8,192-token budget). Layout, shading, and bold as in Table 1.

		Controls			GAMESMITH
Benchmark	Base	Format	Non-game	SPIRAL	matched
Mathematics	32.5	10.7	40.6	39.6	**45.7**
AIME	5.0	0.0	16.7	14.2	**20.8**
AMC	37.0	13.0	44.0	44.0	**51.8**
MATH-500	63.2	21.1	75.5	73.4	**79.4**
Minerva Math	23.9	12.2	31.2	30.8	**32.8**
OlympiadBench	33.1	7.1	35.4	35.7	**43.6**
Knowledge	42.9	34.5	47.4	48.3	**49.6**
MMLU-Pro	52.2	31.9	**62.3**	59.9	61.1
GPQA-Diamond	33.6	37.0	32.4	36.7	**38.0**
Logical reasoning	54.9	50.9	84.1	**85.5**	83.4
BBH Logical Deduction (3 obj.)	51.1	64.0	**97.7**	95.3	95.4
BBH Logical Deduction (5 obj.)	38.4	46.5	**83.8**	81.8	83.4
BBH Web of Lies	75.1	42.1	70.7	**79.5**	71.4
Spatial & tracking	59.5	33.1	**80.4**	78.8	78.4
BBH Tracking Shuffled Objects	74.2	23.5	**96.9**	90.9	87.4
BBH Geometric Shapes	40.3	23.3	50.7	55.7	**56.5**
BBH Navigate	64.0	52.5	**93.6**	89.7	91.4
Average (13 benchmarks)	45.5	28.8	60.8	60.6	**62.5**

Table 16: Per-benchmark results for Qwen3-8B-Base (pass@1 %, 8,192-token budget). Layout, shading, and bold as in Table 1.

		Controls			GAMESMITH
Benchmark	Base	Format	Non-game	SPIRAL	matched
Mathematics	37.4	7.2	44.4	50.5	**51.6**
AIME	10.8	0.0	20.0	25.0	**26.7**
AMC	44.6	6.6	49.4	57.5	**62.0**
MATH-500	69.8	15.6	79.9	84.8	**85.0**
Minerva Math	25.9	9.2	33.1	**36.3**	33.5
OlympiadBench	35.8	4.6	39.4	48.9	**50.4**
Knowledge	48.5	4.3	55.4	56.9	**58.4**
MMLU-Pro	56.8	3.3	**68.7**	68.0	68.7
GPQA-Diamond	40.2	5.3	42.2	45.7	**48.1**
Logical reasoning	78.1	25.0	94.7	90.8	**95.4**
BBH Logical Deduction (3 obj.)	83.6	35.2	**98.6**	96.4	97.8
BBH Logical Deduction (5 obj.)	63.0	12.3	**93.4**	88.2	93.3
BBH Web of Lies	87.7	27.6	92.2	87.9	**95.0**
Spatial & tracking	59.0	17.6	**85.6**	83.4	84.2
BBH Tracking Shuffled Objects	51.1	1.8	**99.1**	95.8	89.5
BBH Geometric Shapes	38.0	3.4	60.1	58.2	**66.0**
BBH Navigate	87.9	47.7	**97.7**	96.2	97.2
Average (13 benchmarks)	53.5	13.3	67.2	68.4	**70.3**

Table 17: Per-benchmark results for Mistral-Nemo-Instruct-2407 (pass@1 %, 8,192-token budget). Layout, shading, and bold as in Table 1.

		Controls			GAMESMITH
Benchmark	Base	Format	Non-game	SPIRAL	matched
Mathematics	16.1	2.1	**19.6**	12.3	17.2
AIME	0.8	0.0	0.8	0.8	**3.3**
AMC	**16.3**	3.6	15.7	7.5	15.1
MATH-500	40.0	2.1	**50.1**	31.6	38.8
Minerva Math	13.1	3.9	**15.2**	11.4	14.3
OlympiadBench	10.6	1.2	**16.5**	10.3	14.4
Knowledge	34.1	2.3	**41.2**	28.4	33.4
MMLU-Pro	35.9	1.3	**52.8**	40.0	46.7
GPQA-Diamond	**32.2**	3.3	29.7	16.9	20.1
Logical reasoning	70.0	14.5	**93.9**	76.5	80.3
BBH Logical Deduction (3 obj.)	85.2	30.0	**98.9**	91.7	96.0
BBH Logical Deduction (5 obj.)	59.1	13.6	**92.8**	74.2	82.7
BBH Web of Lies	65.8	0.0	**90.1**	63.7	62.1
Spatial & tracking	66.9	16.9	**78.4**	69.0	76.2
BBH Tracking Shuffled Objects	83.1	22.3	**99.8**	91.6	95.1
BBH Geometric Shapes	42.7	7.6	41.8	30.7	**46.8**
BBH Navigate	75.0	20.9	**93.6**	84.6	86.7
Average (13 benchmarks)	43.1	8.4	**53.7**	42.7	47.9

Table 18: Per-benchmark results for GLM-4-9B-0414 (pass@1 %, 8,192-token budget). Layout, shading, and bold as in Table 1.

		Controls			GAMESMITH
Benchmark	Base	Format	Non-game	SPIRAL	matched
Mathematics	32.2	2.7	34.5	38.5	**40.3**
AIME	11.7	0.0	10.0	11.7	**15.8**
AMC	30.1	1.5	34.6	41.0	**42.5**
MATH-500	64.8	5.9	71.0	73.0	**75.3**
Minerva Math	25.5	4.6	26.7	**28.8**	27.9
OlympiadBench	29.1	1.6	30.1	38.3	**39.8**
Knowledge	48.1	12.4	48.1	48.2	**50.1**
MMLU-Pro	60.9	13.8	**63.2**	61.2	**63.2**
GPQA-Diamond	35.2	11.0	33.0	35.2	**37.0**
Logical reasoning	86.3	33.5	94.5	92.8	**95.0**
BBH Logical Deduction (3 obj.)	92.0	63.8	**99.3**	98.2	98.3
BBH Logical Deduction (5 obj.)	68.0	35.5	88.5	87.1	**91.9**
BBH Web of Lies	**98.9**	1.1	95.6	93.0	94.9
Spatial & tracking	63.4	30.5	83.8	82.6	**86.4**
BBH Tracking Shuffled Objects	47.0	24.2	**99.4**	98.0	97.3
BBH Geometric Shapes	53.9	9.6	55.7	57.7	**67.9**
BBH Navigate	89.3	57.8	**96.4**	92.2	93.9
Average (13 benchmarks)	54.3	17.7	61.8	62.7	**65.1**

Table 19: Generation-level diagnostics for the Format control, macro-averaged over the 13 benchmarks of Table 1 (%). Avg. is the 13-benchmark mean of Table 1, and the remaining columns are defined in the text.

Model	Setting	Avg. (13)	Answer-first	Action-shaped
Qwen3-4B-Base	Base	45.5	1.0	0.0
	Format	28.8	99.9	0.0
	GAMESMITH	62.5	0.0	0.0
Qwen3-8B-Base	Base	53.5	0.5	0.0
	Format	13.3	99.9	68.5
	GAMESMITH	70.3	0.0	0.0
Mistral-Nemo-Instruct-2407	Base	43.1	0.0	0.0
	Format	8.4	99.6	68.3
	GAMESMITH	47.9	0.0	0.0
GLM-4-9B-0414	Base	54.3	0.0	0.0
	Format	17.7	98.7	79.4
	GAMESMITH	65.1	0.0	0.0

0.6, top-p 0.95). We measure two quantities, each macro-averaged over the 13 benchmarks: the share of samples that open a `\boxed{}` within the first 32 characters (Answer-first), and the share of answered samples whose answer is wrapped in square brackets in the manner of a game action (Action-shaped). The Qwen3-4B-Base rows come from a re-run of its three settings under the same protocol, since the original runs kept no per-sample outputs. This re-run reproduces the means of Table 1 to within 0.4 points, and the Avg. column keeps the values of Table 1.

We observe that the Format control emits its answer as its first tokens. On the three larger models the answer frequently takes the shape of a game action, whereas on Qwen3-4B-Base the answer is a bare letter or number. These results indicate that supervising the format without the reasoning removes the base model's own reasoning rather than adding to it. The Format column therefore records the direction and mechanism of this loss rather than a level of ability, since several of the multiple-choice benchmarks fall to or below chance.

D.4 ESTIMATOR COMPARISON WITH ONE EPISODE PER VARIANT

The self-play runs of Table 2 play every sampled variant $G = 5$ times per optimiser step, so that both estimators see the same batches. In this section, we examine what remains of the difference between the two estimators when each variant is played once ($G = 1$). With one episode per variant there is no group to average over: RAE reduces to its running mean per variant and seat, and CRAB reduces to the prior m_g of equation 4, because $K'_g = 0$ in equation 4 and the leave-one-out term vanishes. The comparison therefore isolates the two sources of equation 4 that do not depend on the current batch: a per-variant running mean against a prior fitted across the corpus.

Both runs start from the GAMESMITH distillation checkpoint, use the same corpus, sampler, token budget, and learning rate as the main runs (Appendix C.2), and differ from them only in G. The batch of 128 transitions is kept, so a $G = 1$ step covers five times as many distinct variants as a $G = 5$ step. Checkpoints are selected as in Table 2, Table 20 reports the results, and Figure 5b follows the Qwen3-4B-Base runs across the budget.

We make three observations. First, the prior alone retains the advantage of CRAB: with $G = 1$, CRAB exceeds RAE on every model, by 1.6 points on Qwen3-4B-Base, 1.0 on Qwen3-8B-Base, 3.1 on Mistral-Nemo-Instruct-2407, and 0.6 on GLM-4-9B-0414, and it improves on the distilled model on every model, as with $G = 5$. Second, CRAB is insensitive to the group size, whereas RAE is not. Its $G = 1$ scores are within 0.3 points of its $G = 5$ scores in Table 2 on every model, while RAE loses 1.8 points on Mistral-Nemo-Instruct-2407 when each variant is played once. Third, Figure 5b shows on Qwen3-4B-Base the same behaviour over the budget as with $G = 5$: CRAB is above its starting point from the first evaluated checkpoint and ends 2.5 points above it, whereas RAE peaks at step 20, falls below the starting point for most of the budget, and recovers only towards the end. Since a $G = 1$ step covers five times as many distinct variants, these results indicate that

the prior, which is defined on every variant, is what allows the estimator to make use of the breadth of the corpus.

Table 20: Self-play with one episode per variant ($G = 1$) on the GAMESMITH corpus (13-benchmark mean pass@1 %). Both runs start from the GAMESMITH distillation checkpoint of Table 2 and differ only in the estimator. Bold marks the higher of the two RL runs in each row.

Model	Distill.	+RL (RAE, $G = 1$)	+RL (CRAB, $G = 1$)
Qwen3-4B-Base	62.5	63.4	**65.0**
Qwen3-8B-Base	70.3	71.8	**72.8**
Mistral-Nemo-Instruct-2407	47.9	45.5	**48.6**
GLM-4-9B-0414	65.1	64.7	**65.3**

D.5 EVALUATION CURVES DURING SELF-PLAY RL

Figure 5 shows the self-play curves on Qwen3-4B-Base, and its top panel (Figure 5a) follows the three self-play pipelines of Table 2 across the whole budget. We make three observations. First, the CRAB pipeline stays above its distillation checkpoint at every evaluated step, and its gain is concentrated on mathematics and logical reasoning, where it ends 2.3 and 4.6 points above the starting point. Second, RAE on the same corpus and checkpoint falls below the starting point by step 40 and returns to it only at the end of the budget. The fall is driven by the knowledge group, where it loses more than five points by step 120 before recovering. This is the behaviour anticipated in §1 and §4.2: a baseline kept separately for each variant is unreliable when a run visits each variant only a few times, so self-play with RAE on the synthesised corpus is harmful for most of the budget, and the two RAE pipelines end level in Table 2 although the GAMESMITH one starts 1.9 points higher, whereas the SPIRAL pipeline, which replays three games, gains steadily from its lower start. Third, the two groups that the games exercise least are the least affected by the estimator: knowledge moves by at most two and a half points under the CRAB and SPIRAL pipelines, and spatial and state tracking fluctuates around the starting point under CRAB and falls below it under RAE on either corpus. The picture is similar when every sampled variant is played once: Figure 5b repeats the comparison at $G = 1$ with the runs of Appendix D.4 and shows the same ordering of the three pipelines.

D.6 DRAWS AND THE REWARD SIGNAL

A zero-sum game can end in a draw, and a draw returns 0 to both seats. A natural concern is that self-play drifts into draws and thereby loses its reward signal, as happens on Tic-Tac-Toe once both sides play well enough. Two mechanisms limit this effect, and Table 21 reports what happened in the runs of Table 2.

The first mechanism is admission. The fingerprint of random play excludes a game that produces only draws, and the playability test requires at least 25% of episodes between two score-maximising reference bots to be decisive (Appendix A.2). In the admitted corpus, the base game of a family is decisive in at least 69% of random episodes (`crossl`), in at least 90% for 26 of the 29 families, and the median is 1.00. Among the 336 admitted variants, three rule variants draw in nearly every random episode because the pattern that decides the game is rarely completed by random play, and one of them, the `nosqre` variant with a 3×3 losing square, is included in the self-play pool.

The second mechanism is the estimator. A drawn episode is not a lost sample: its return is 0, and equation 1 uses $R(\tau_i) - b_i$, which is nonzero whenever the baseline is not exactly 0. Since CRAB shrinks the leave-one-out mean of the same game towards the prior m_g, b_i differs from $R(\tau_i)$ unless the prior happens to equal it. Table 21 reports the fraction of episodes that were drawn, averaged over the first and the last 20 steps of the budget.

Three observations stand out. First, on the synthesised corpus the draw rate stays between 3% and 15% throughout training on every model, and on Qwen3-4B-Base it decreases under CRAB. Second, on the three SPIRAL games it climbs from about 10% to 25 to 31% by the end of the budget on every model, which is the pattern expected of a small fixed set of games that the policy learns to

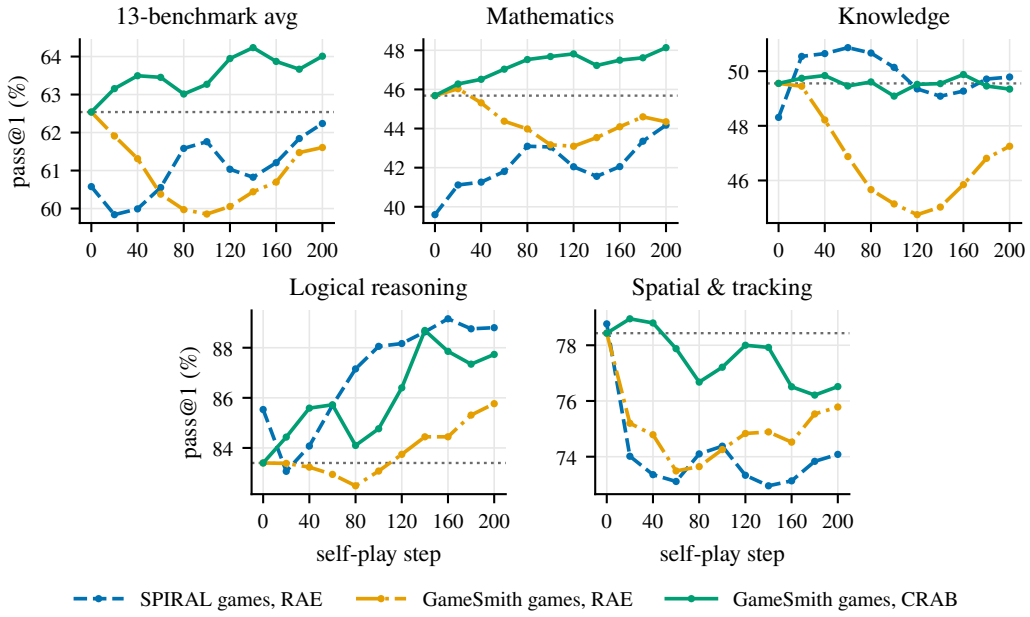

(a) Every sampled variant played $G = 5$ times per step, the runs of Table 2.

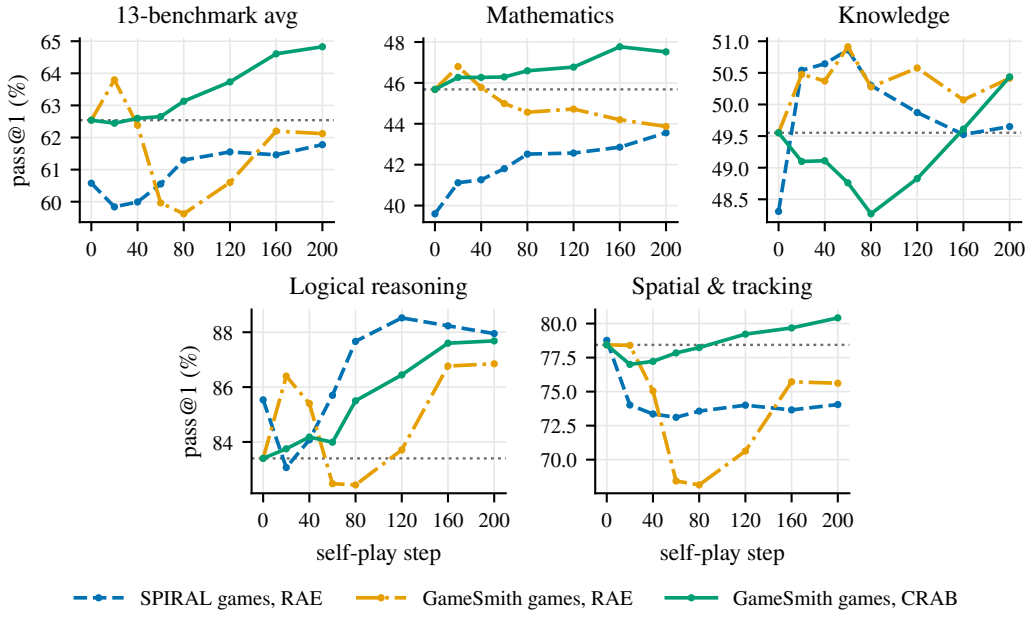

(b) Every sampled variant played once ($G = 1$): the two GAMESMITH runs of Appendix D.4 and the SPIRAL run of Table 2.

Figure 5: Self-play on Qwen3-4B-Base over the 200-step budget, evaluated at the seven checkpoints of the grid of Table 2, for the 13-benchmark mean and for each capability group (pass@1 %). The dotted line is the GAMESMITH distillation checkpoint from which the two GAMESMITH pipelines start, and the SPIRAL pipeline starts from its own distillation checkpoint.

play to a draw. The concern is therefore real for hand-written games, and it is precisely what the breadth of the corpus removes. Third, we also logged, for the CRAB runs, whose baseline uses the group of episodes of the same variant, the fraction of groups of size at least two whose returns were

all identical: it lies between 4 and 13% across the four models. Even in these groups no advantage is exactly zero (the logged fraction of advantages equal to zero is 0.0 in every run), because the prior term keeps the baseline away from the group's common return, and the state-value term of equation 5 adds a per-decision signal on top. A nonzero advantage is a necessary condition for a gradient signal, not a sufficient one. If every action available in a group leads to the same return, the expected gradient of that group is zero for any action-independent baseline, and a nonzero baseline only adds a zero-mean term to the update. The quantities that bear on the signal are therefore the draw rate and the fraction of same-return groups, which bound the share of the batch that can carry no signal, whereas the absence of zero advantages rules out only the degenerate case of a batch of draws that contributes nothing at all to the gradient. Whether the remaining advantages carry signal is a question about policy improvement, not about the advantages themselves.

Table 21: Draw rate during self-play, from the training logs of the runs of Table 2, steps 1 to 200.

Model	Games	Estimator	Draw rate (%)	
			first 20 steps	last 20 steps
Qwen3-4B-Base	SPIRAL	RAE	7.1	25.0
	GAMESMITH	RAE	5.7	10.9
	GAMESMITH	CRAB	7.4	5.3
Qwen3-8B-Base	SPIRAL	RAE	9.5	30.7
	GAMESMITH	RAE	4.2	15.2
	GAMESMITH	CRAB	4.3	14.2
Mistral-Nemo-Instruct-2407	SPIRAL	RAE	12.7	29.4
	GAMESMITH	RAE	3.4	10.8
	GAMESMITH	CRAB	3.6	11.8
GLM-4-9B-0414	SPIRAL	RAE	9.9	30.7
	GAMESMITH	RAE	3.0	12.5
	GAMESMITH	CRAB	2.7	11.1

D.7 WIN RATES ON HELD-OUT VARIANTS

The benchmarks of Table 2 measure transfer. In this section, we examine whether the self-play runs also play the games better. We compare the two pipelines that differ in both the corpus and the estimator, namely SPIRAL games with RAE and GAMESMITH games with CRAB, at the checkpoints selected for Table 2 (Table 22).

The test set consists of 54 variants that neither pipeline was trained on: for 18 of the 29 families, one variant on each of the encoding, rule, and size axes of Appendix A.4. Every variant is played for 40 episodes, 20 from each seat, with the same budget and sampling as training. The opponent is Qwen3-4B-Instruct under the same budget, and the two pipelines are also played against each other on the same positions. An invalid move or a reply that runs to the budget counts as a loss. The 40 episodes of a variant form 13 best-of-three series, and each cell reports the share of series won, so that 50 corresponds to parity with the opponent.

Table 22b shows that the GAMESMITH pipeline plays better than the SPIRAL pipeline. Against Qwen3-4B-Instruct it wins 42.5% of the series overall against 33.5%, and head-to-head it wins 62.7%. The gap is concentrated on the grid genre, where the GAMESMITH pipeline wins 40.6% of the series against 18.4%: the SPIRAL pipeline loses a quarter of its grid games by moving to an occupied cell or by running past the budget, both of which count as losses, and it wins only 26% of the head-to-head series on grid. The two pipelines are level on negotiation, and the gap on card is within a few points. Table 22a repeats the protocol on the two distillation checkpoints from which the pipelines start, and the ordering is the same before any self-play: distillation from the synthesised games plays better than distillation from the three SPIRAL games on every genre, by the largest margin on grid. The ordering of the self-play pipelines is therefore inherited from their starting points and preserved by the self-play stage.

Table 22: Playing strength on the held-out variants, as the share of best-of-three series won (%). The first four columns play against Qwen3-4B-Instruct under the training budget, and the last column of (b) plays the two self-play pipelines against each other. An invalid move or a reply that runs to the token budget counts as a loss. Bold marks the higher value in each column.

(a) The two distillation checkpoints from which the self-play pipelines start, before any self-play.

	vs. Qwen3-4B-Instruct			
Distilled on	Card	Grid	Negotiation	All
SPIRAL games	34.1	12.8	32.7	26.7
GAMESMITH games	**40.1**	**36.8**	**43.6**	**39.7**

(b) The self-play pipelines of Table 2 at their selected checkpoints.

	vs. Qwen3-4B-Instruct				Head-to-head
Self-play pipeline	Card	Grid	Negotiation	All	series won
SPIRAL games, RAE (step 200)	36.2	18.4	**51.0**	33.5	37.3
GAMESMITH games, CRAB (step 120)	**40.7**	**40.6**	48.7	**42.5**	**62.7**
Series per column	312	234	156	702	702

E SYNTHESIS PROMPTS

The designer and the engineer are the same generator model, namely GPT-5 accessed through its API with the provider's default sampling. The designer receives up to 32,768 completion tokens and the engineer up to 24,576. An engineer implementation that fails a replay test receives the test output verbatim and is revised, for at most five attempts. The system prompts of both roles for the three templates, the user messages that instantiate them, and the playtest prompt are reproduced below verbatim from the synthesis code. Braces mark values that are filled in at run time.

Designer system prompt, grid-placement template

```
You are a game designer for an RL research pipeline. Propose NEW two-player, zero-sum, turn-based GRID
  PLACEMENT games implementable in a fixed skeleton (players alternate placing marks on a grid; game
  logic only controls: which cells are legal, what placing does, and when someone wins/loses/draws).
   The
   games must be DIFFERENT from standard Tic-Tac-Toe and from each other, deterministic,
  perfect-information, and end within ~50 moves.

Good mechanic directions: misere/anti variants, Notakto, Order&Chaos, Domineering-style blocking,
  connection goals, custodial capture, majority-of-lines scoring, forbidden patterns.

HARD RULE: define player roles and objectives by MOVE ORDER (the first player / the second
player), NEVER by display symbols or labels -- those are cosmetic and get randomized.

Return a JSON list; each item:
{"key": "SHORTKEY (<=6 uppercase letters)",
 "name": "...",
 "rules": "complete, unambiguous natural-language rules a strong player could play from",
 "semantic_knobs": {"knob_name": "meaning + sensible int/bool values"},
 "deduction_note": "why strong play requires verifiable step-by-step deduction (1-2 sentences)"}
```

Designer system prompt, betting-with-showdown template

```
You are a game designer for an RL research pipeline. Propose NEW two-player, zero-sum BETTING/SHOWDOWN
  card games implementable in a fixed skeleton. The skeleton is sealed: it deals each player hidden
  cards from a deck of ranks, runs a standard limit-betting round (check/bet/call/fold/raise), and
  settles chips. THE ONLY THING EACH GAME CONTROLS IS THE HAND RANKING FUNCTION: given a player's cards
   ,
   compute a comparable strength value (higher wins the showdown; ties split). Games must differ from
  plain Kuhn poker (highest card wins) and from each other via genuinely different ranking logic.

Good directions: lowball, middle-card-wins, sum modulo N, pair/duplicate bonuses, distance between
  cards, parity-based rankings, "closest to target sum without exceeding it".
```

```
Knobs may include deck size, hand size, ante, bet size, plus ranking-specific parameters.

HARD RULE: define player roles and objectives by MOVE ORDER (the first player / the second
player), NEVER by display symbols or labels -- those are cosmetic and get randomized.

Return a JSON list; each item:
{"key": "SHORTKEY (<=6 uppercase letters)",
 "name": "...",
 "rules": "complete, unambiguous natural-language rules a strong player could play from",
 "semantic_knobs": {"knob_name": "meaning + sensible int/bool values"},
 "deduction_note": "why strong play requires verifiable step-by-step deduction (1-2 sentences)"}
```

Designer system prompt, resource-negotiation template

```
You are a game designer for an RL research pipeline. Propose NEW two-player RESOURCE-NEGOTIATION games
  implementable in a fixed skeleton that generalizes SimpleNegotiation. The skeleton is sealed: it
   deals
   each player quantities of several resource types plus a PRIVATE per-unit value for each type;
   players
   alternate turns; on your turn you either propose ONE trade from a listed menu of concrete swaps, or
  accept/refuse the opponent's pending proposal; accepted trades move the goods. Settlement is ZERO-SUM
   :
   whoever's inventory SCORE grew more by the final turn wins (equal growth = draw).

THE ONLY THING EACH GAME CONTROLS IS HOW AN INVENTORY BECOMES A SCORE (and optionally which swaps are
   on
   the menu). Plain SimpleNegotiation scores an inventory as sum(quantity x private unit value); your
  games must differ via genuinely different scoring structure, so that which trades are worth making
  changes qualitatively.

Good directions: diminishing returns (each extra unit of a type is worth less), SET-COLLECTION bonuses
  (points for holding at least k of every type), complementary pairs (a bonus per matched pair across
  two specific types), threshold/quota bonuses (a jump once a type crosses a level), monopoly bonuses
  (holding the majority of a type), caps (units beyond a cap score nothing), parity or spread bonuses
  (rewarding balance across types instead of hoarding one).

CRITICAL: the game must stay non-degenerate under RATIONAL play -- mutually beneficial trades must
   EXIST
   (both sides can gain because their private values and holdings differ), otherwise a rational pair
  never trades and every game is a draw. Say in the rules why a rational opponent would ever accept a
  proposal.
Knobs may include resource count, turn budget, valuation spread, trade scale, plus scoring-specific
  parameters (bonus size, threshold level, set size, cap).

HARD RULE: define player roles and objectives by MOVE ORDER (the first player / the second
player), NEVER by display symbols or labels -- those are cosmetic and get randomized.

Return a JSON list; each item:
{"key": "SHORTKEY (<=6 uppercase letters)",
 "name": "...",
 "rules": "complete, unambiguous natural-language rules a strong player could play from",
 "semantic_knobs": {"knob_name": "meaning + sensible int/bool values"},
 "deduction_note": "why strong play requires verifiable step-by-step deduction (1-2 sentences)"}
```

Designer user message

```
Propose {n} games. Existing corpus already has: {list of admitted games on this template}. Avoid
  near-duplicates of these. Output ONLY the JSON array (in a ```json fence), no prose.
```

Engineer system prompt, grid-placement template

```
You implement a two-player grid game inside a FIXED skeleton. You may ONLY write:
1) a frozen dataclass `Config(GridConfig)` adding the game's semantic knobs (with defaults);
2) a class `Game(GridGameBase)` implementing ONLY these hooks (all in CANONICAL coordinates):
   - legal_moves(self, board, pid, extras) -> list[(r,c)]   (optional; default = empty cells)
   - apply_move(self, board, pid, r, c, extras) -> None      (optional; default = board[r][c]=pid)
   - outcome(self, board, pid, r, c, extras) -> None | ("win", pid) | ("lose", pid) | ("draw",)
     called right after pid placed at (r,c); ("lose", pid) means the MOVER loses.
   - rules_text(self, cfg, player_id, symbols) -> str        (clear rules; mention both symbols)
   - init_extras(self) -> dict                               (optional per-episode state)
```

```
3) a `make_suite(cfg_cls)` returning {"train": [cfgs], "val": [cfgs], "test": [cfgs]} where train
   uses randomize_codec=True and test holds out symmetry="transpose" plus one rule-knob variant;
4) the closing `globals().update(family_boilerplate(KEY, __name__, Game, Config,
   semantic_fields=(...), suite_fn=make_suite))`.
Board stores None / 0 / 1 (player ids) ONLY -- never symbols. Do not touch rendering, parsing,
codecs, textarena, or the State machinery. The game must always terminate (the skeleton
auto-draws when neither player has legal moves).
HARD RULES: deterministic logic only (no randomness in hooks, no I/O, no clock). Imports allowed:
  dataclasses, typing, math, itertools, and the skeleton import shown above. Hooks COMPUTE, they never
  render or print. rules_text must describe the rules using the provided labels argument, never
  hardcoded display strings. Your Config MUST override structural defaults (board/deck/hand/slot sizes)
  to the values the SPEC intends -- do NOT inherit skeleton defaults; the game's mechanic must be
  non-degenerate at the Config defaults (a behavioral-duplicate gate will reject games that collapse to
  an existing ordering). Output ONE ```python block, nothing else.
```

Engineer system prompt, betting-with-showdown template

```
You implement a betting/showdown card game inside a FIXED skeleton. You may ONLY write:
1) a frozen dataclass `Config(CardConfig)` adding the game's semantic knobs (with defaults);
2) a class `Game(CardGameBase)` implementing ONLY these hooks:
   - hand_value(self, hand, cfg) -> comparable value (int or tuple; HIGHER wins the showdown,
     equal values split the pot). `hand` is a list of int ranks in [0, cfg.n_ranks).
   - rules_text(self, cfg, player_id, labels) -> str. `labels` is a dict with the current
     display words for actions ('check','bet','call','fold','raise') and labels['ranks'] =
     rank labels low-to-high. Explain the ranking rule precisely using these labels.
3) a `make_suite(cfg_cls)` returning {"train": [cfg_cls(randomize_codec=True)],
   "val": [cfg_cls(rank_scheme="number", action_scheme="formal")],
   "test": [cfg_cls(rank_scheme="letter", action_scheme="casual"), <one rule-knob variant>]};
4) the closing `globals().update(card_family_boilerplate(KEY, __name__, Game, Config,
   semantic_fields=(...), suite_fn=make_suite))`.
Import: from driftgym.skeletons.card_game import CardConfig, CardGameBase, card_family_boilerplate
Do not touch dealing, betting flow, chips, rendering, or State machinery.
HARD RULES: deterministic logic only (no randomness in hooks, no I/O, no clock). Imports allowed:
  dataclasses, typing, math, itertools, and the skeleton import shown above. Hooks COMPUTE, they never
  render or print. rules_text must describe the rules using the provided labels argument, never
  hardcoded display strings. Your Config MUST override structural defaults (board/deck/hand/slot sizes)
  to the values the SPEC intends -- do NOT inherit skeleton defaults; the game's mechanic must be
  non-degenerate at the Config defaults (a behavioral-duplicate gate will reject games that collapse to
  an existing ordering). Output ONE ```python block, nothing else.
```

Engineer system prompt, resource-negotiation template

```
You implement a two-player resource-NEGOTIATION game inside a FIXED skeleton. You may ONLY write:
1) a frozen dataclass `Config(NegConfig)` adding the game's semantic knobs (with defaults) AND
   overriding structural knobs (n_resources, max_turns, qty_min, qty_max) to what the SPEC intends;
2) a class `Game(NegGameBase)` implementing ONLY these hooks (all COMPUTE-only, never render):
   - inventory_score(self, quantities, values, cfg) -> int   THE MECHANIC. `quantities` is a list of
     ints indexed by canonical resource index (0=cheapest .. n-1=dearest base value) and `values` is
     that player's private per-unit values, same indexing. Return an int score. Default = sum(q*v).
     Must be deterministic and pure. Higher = better for that player.
   - menu(self, cfg) -> list[(give_idx, get_idx, give_qty, get_qty)]   (optional) the proposable
     swaps, in a STABLE order (canonical actions are `offer {k}` by list index). The skeleton default
     lists every ordered resource pair at BASE-VALUE PARITY (gcd ratios, e.g. 8 units of a 5-value
     resource for 1 unit of a 40-value one). KEEP PARITY-LIKE RATIOS: equal-quantity swaps across an
     unequal value ladder make every proposer-favourable trade harmful to the responder, so a
     rational pair never trades and the game degenerates to a guaranteed draw.
     WARNING: HARD GATE (certificate C-rational): a reference bot that greedily maximizes ITS OWN score
     plays both seats; the game FAILS unless it executes >=0.5 trades/episode and >=25% of episodes
     are decisive. The skeleton's DEFAULT menu is parity in the *base* values, so if your
     inventory_score is strongly non-linear (steep diminishing returns, big set/quota/variance
     bonuses) those swaps are LOSS-MAKING for both sides under your own scoring and nothing ever
     trades. Two ways to satisfy the gate: (i) keep the non-linearity MILD so that score stays close
     to monotone in base value (bonuses small relative to sum(q*v)), or (ii) override menu() so the
     quantities are parity under YOUR scoring rule at typical inventories. State in rules_text why a
     rational opponent would accept.
   - trade_ok(self, give_idx, get_idx, gq, rq, quantities, cfg) -> bool   (optional; default = the
     proposer holds at least gq of give_idx)
   - rules_text(self, cfg, player_id, labels) -> str   describe the scoring rule precisely using
     labels['resources'] (display names), labels['base_values'], and labels['offer'/'accept'/'deny'].
3) a `make_suite(cfg_cls)` returning {"train": [cfg_cls(randomize_codec=True), ...],
   "val": [cfg_cls(resource_scheme="num", action_scheme="alt")],
   "test": [cfg_cls(resource_scheme="minerals", action_scheme="market"), <one rule-knob variant>,
            <one structural variant>]};
```

```
4) the closing `globals().update(neg_family_boilerplate(KEY, __name__, Game, Config,
   semantic_fields=(...), suite_fn=make_suite))`.
Import: from driftgym.skeletons.negotiation_game import NegConfig, NegGameBase, neg_family_boilerplate
Settlement is zero-sum and owned by the skeleton (it compares each side's score growth) -- do not
touch dealing, the offer state machine, trade execution, rendering, or State machinery.
HARD RULES: deterministic logic only (no randomness in hooks, no I/O, no clock). Imports allowed:
  dataclasses, typing, math, itertools, and the skeleton import shown above. Hooks COMPUTE, they never
  render or print. rules_text must describe the rules using the provided labels argument, never
  hardcoded display strings. Your Config MUST override structural defaults (board/deck/hand/slot sizes)
  to the values the SPEC intends -- do NOT inherit skeleton defaults; the game's mechanic must be
  non-degenerate at the Config defaults (a behavioral-duplicate gate will reject games that collapse to
  an existing ordering). Output ONE ```python block, nothing else.
```

Engineer user message (first attempt)

```
SKELETON SOURCE (read the base class contract):
```python
{template source file}
```

REFERENCE IMPLEMENTATION on this skeleton:
```python
{hand-written seed game of the template}
```

Now implement THIS game. KEY={KEY}. module will be driftgym.corpus.{key}.env
SPEC:
{designer specification as JSON}
```

Engineer user message (repair, appended after each failed attempt)

```
Attempt {k} FAILED:
{verbatim output of the failing replay tests, or the traceback}

Fix the implementation. Output the complete corrected file as ONE ```python block.
```

Independent re-implementation user message (same engineer system prompt; the first implementation is not shown)

```
SKELETON SOURCE (read the base class contract):
```python
{template source file}
```

Now implement this game FROM ITS SPEC alone. KEY={KEY}T. module will be driftgym.corpus.{key}.twin_env
Use EXACTLY these Config defaults (field names and values):
{Config defaults of the first implementation as JSON}

SPEC:
{designer specification}
```

Playtest system prompt (the model plays one seat; the user message is the rules text and the current observation)

```
You are playing a two-player game. Read the rules and current state, then move.
Reply with EXACTLY one line: [label] | END: win  or  [label] | END: lose  or
[label] | END: draw  or  [label] | END: none
END states what happens to YOU immediately after this move by the rules: win/lose/draw if the game ends
  now, none if it continues. Choose the strongest legal move.
```